Danish Meteorological Institute
Ministry of Transport and Energy

Technical Report 05-12

DMI-HIRLAM Modelling with High Resolution Setup and Simulations for Areas of Denmark

Alexander Mahura, Kai Sattler, Claus Petersen,
Bjarne Amstrup, Alexander Baklanov

Copenhagen 2006

Colophon

Serial title:
Technical Report 05-12

Title:
DMI-HIRLAM Modelling with High Resolution Setup and Simulations for Areas of Denmark

Subtitle:

Author(s):
Alexander Mahura, Kai Sattler, Claus Petersen, Bjarne Amstrup, Alexander Baklanov

Other contributors:

Responsible institution:
Danish Meteorological Institute

Language:
English

Keywords:
DMI-HIRLAM, climate generation, land use, high resolution modelling, ISBA

Url:
www.dmi.dk/dmi/tr05-12

ISSN:
1399-1388

Version:
27 June 2005

Website:
www.dmi.dk

Content:

Abstract

In this technical report the results of the DMI-HIRLAM (U01) research high resolution (1.4 km) model simulations during spring-summer of 2005 are analysed. The high resolution model domains used in research activities of DMI are outlined; their results of land use classification and climate generation are presented. The ISBA land surface scheme is tested in more details for specific dates by modifying the parameters of roughness, albedo and anthropogenic heat fluxes over urbanized cells of domain. The outputs for models of U01 and S05 vs. observational data are compared. The diurnal cycles of temperature and humidity at 2 m, wind velocity at 10 m, and mean sea level pressure are estimated based on long-term simulations. From these outputs, two specific dates of typical and low winds are also evaluated.

Resumé

I denne tekniske rapport vil en test version af DMI-HIRLAM (U01) blive beskrevet. Den horisontale opløsning af modellen er 1.4 kilometer men er ellers identisk med den operationelle version af DMI-HIRLAM bortset fra model domain og tidsskrift. En detaljeret beskrivelse af de data der beskriver overfladebeskaffenheden for DMI-HIRLAM bliver gennemgået og modellens sensivitet over for variation i nogle af disse parametre her i blandt rughed, albedo, antropogenisk varmefluks over urbane områder bliver testet. Output fra U01 er sammenlignet med S05 og observation over en lang periode og der er særligt lagt vægt på at verificere den daglige gang af overfladeparametrene: temperatur og dugpunktstemperatur i 2 meters højde, 10 meter vind hastighed og overfladetryk reduceret til havniveau. Derudover bliver 2 situationer, hvor svage vinde er dominerende, grundigt gennemgået.

1. Introduction

Physiographic data influencing through the air-surface interactions play an important role in any numerical weather prediction (NWP) modelling. These data serve as low boundary conditions of the NWP modelling domains and include parameters of geographical distribution on a 2D plane of terrain, land use, soil types, and other various properties. All these have influence on the structure and behaviour of the surface and mixing layers of atmosphere, as well as spatial and temporal distribution of main meteorological variables such as temperature, wind characteristics, humidity, etc. Depending on resolution and scales of model domains (high vs low resolution, meso vs large scale, etc.), different datasets can be used as input for processing of climate generation for NWP. For example, for the DMI HIgh Resolution Limited Area Model (HIRLAM) (*Sass et al., 2002*), the Global 30 Arc Elevation Data, GTOPO30 (*USGS, 1998*); Global Land Cover Characteristics, GLCC (*USGS,1997*); CORINE, and other datasets can be used. In general, several steps – 1) definition of boundaries and parameters of new modelling domains for NWP, 2) preprocessing of physiographic data, and 3) production of climate generation files (CGFs) - for such domain are done apriori. It is due to computational expenses, and moreover, since it is needed to be done only once. The output generally consists of 12 CGFs (one file for each month) having physiographic and climatic characteristics for each grid cell of the model domain. Two formats are available. The inputs are files having the hierarchical data format (HDF) allowing minimized sizes of output files and unified formats. These files can be viewed using HDFLook software package (*NCSA, 1999ab*). The GRIdded Binary (GRIB) format files are output of the climate generation and read directly by the HIRLAM model at initialization step. GRIB serves as a data storage format, generating the same efficiencies relative to information storage and retrieval devices. These files can be viewed using METGRAF software package (*Mogensen, 2004; METGRAF*). Detailed information on these formats can be found in *NCSA (1999ab)* and *WMO (1994)*, respectively.

The detailed procedure of physiographic processing and climate generation for several versions of the DMI-HIRLAM models with resolutions of more than 0.05 degrees is given by *Sattler (1999).* Previously some tests of DMI-HIRLAM on high resolution were done for the verification forecasts and urban meteorology within the FUMAPEX project (*Baklanov et al., 2002; Amstrup, 2004; Baklanov et al., 2004; Fay et al., 2005*) on examples of area of the Island of Zeeland and other Danish territories, and cities of Helsinki, Oslo, and Bologna. In this report, the focus is on the high resolution modelling research domains used by DMI-HIRLAM. For the new domains, a series of DMI-HIRLAM high resolution simulations during spring-summer of 2005 as well as for summer of 2004 were performed and then analyzed.

2. Definition of Modelling Domain

The new high resolution domain for the DMI-HIRLAM-**U01** research version includes the territory of mainland Denmark with the island of Bornholm, the northernmost border territories of Germany, and the south-western territories of Sweden - as shown in Fig. 2.1a. The DMI-HIRLAM-**I01** research version is focused on the Island of Zeeland (as shown in Fig. 2.1b) and mostly oriented for study and evaluation of effects of urbanized areas (such as Copenhagen metropolitan area) on formation and evolution of meteorological fields within the surface and atmospheric boundary layers.

The U01 modeling domain is represented in the rotated system of coordinates, where the selected south pole latitude is –40 degrees, and the pole longitude is 10 degrees. Similarly, I01 is also given in such a system of coordinates, but with the south pole latitude at 0 degrees and longitude at 100 degrees. For both domains the south, west, north, and east boundaries are given also in the rotated system of coordinates (Tab. 2.1). Since in this system one degree is equal approximately to

111.3 km, the horizontal resolutions are equivalent approximately to 1.56 km, respectively. The parameters of the domain sizes are shown in Tab. 2.1. For modeling domain these include the:

1) number of grid points along rotated longitude (NLON);
2) number of grid points along rotated latitude (NLAT);
3) number of vertical levels (NLEV); and
4) total number of passive boundary points from the borders of modeling domain (NBNDRY).

The last with addition of relaxation points (10 from each side of domain) is shown in Fig. 2.1.1a as an inner border (Ubnd) of domain. I.e. the forecasted output by the model will be useful and valuable to analyze for the inner domain, although the entire domain is larger as shown by the outer border (U01). It is the same for the I01 domain. Note, for these U01 and I01 domains with resolution of 0.014 degrees, the total number of grid cells is equal to 96200 and 14632, respectively.

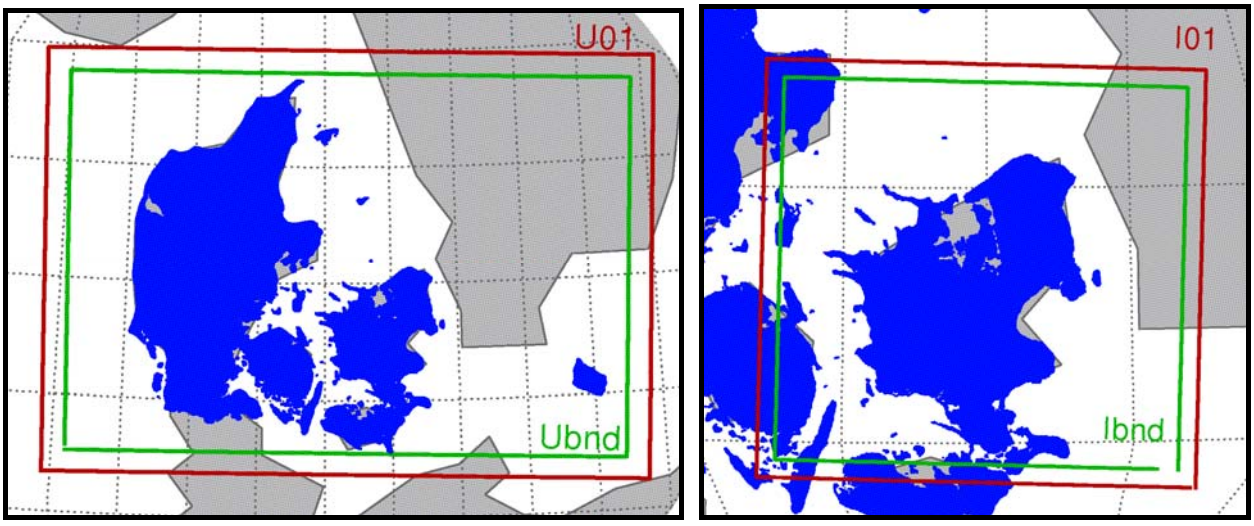

(a) (b)

Fig. 2.1. DMI-HIRLAM (a) U01 and (b) I01 modelling domains with high resolution of 0.014 degrees (1.56 km).

Resolutions (deg / km)	**0.014 / 1.56**	**0.014 / 1.56**
Parameters for domains	**I01**	**U01**
Domain sizes		
NLON	124	370
NLAT	118	260
NLEV	40	40
NBNDRY	10	10
Domain boundaries		
SOUTH	–1.966	4.379
WEST	–35.138	–1.823
NORTH	–0.244	8.005
EAST	–33.500	3.343

Tab. 2.1. Parameters of the DMI-HIRLAM-I01 and U01 modelling domains with high resolutions.

The definition of the new modeling domain (NMD) is the initial preparation step to calculate further the climate generation files for a new domain resolution. The general steps and requirements are given in Appendix 1 on example of the U01 NMD with a resolution of 0.014 degrees. In preparation, several requirements should be satisfied.

First, the horizontal resolution along latitude and longitude should be equal.

Second, both the number of grid points along latitude and longitude need be even numbers.

Third, values of domain boundaries should be given in millidegrees.

Fourth, a set of formulations should be followed in calculations of domain size parameters given in Tab. 2.1:

NBNDRY = 2 (NPBP + 1), where: NPBP- is the number of selected passive boundary points;

$NLON_{NWP} = NLON_{NMD} - NBNDRY$, where subscript NMD is for new modeling domain and subscript NWP is for DMI-HIRLAM model;

$NLON_{NMD} - 1 = | WEST_{NMD} - EAST_{NMD} | / \Delta LON$;

$NLAT_{NMD} - 1 = | NORTH_{NMD} - SOUTH_{NMD} | / \Delta LAT$.

Note, $NLON_{NWP}$ should satisfy also a set of (n, m, p) conditions given by $NLON_{NWP} = (2^{n} \cdot 3^{m} \cdot 5^{p})$ for usage on DMI NEC computer (FFT limitation) (see Table of Appendix 2).

3. Land Use Classification and Climate Generation Pre-processing for Modelling Domain

3.1. General Scheme of Climate Generation for DMI-HIRLAM

The physiographic data are preprocessed. Both elevation and land use data are re-analyzed during preprocessing. In each grid cell of the new modeling domain the elevation is calculated as mean, and land use classes are transformed in accordance to the HIRLAM Interaction Soil Biosphere Atmosphere (ISBA) Land Surface Scheme (LSS) requirements. This scheme is based on original formulations of *Noilhan & Planton, 1989* and *Noilhan & Mahfouf, 1996*.

The climate generation procedure for the DMI-HIRLAM model uses a set of different data sources, including the Global 30 Arc Elevation Data, GTOPO30 (*USGS, 1998*) and Global Land Cover Characteristics, GLCC (*USGS, 1997*) data. The procedure of generation, required routines, detailed performed steps, etc. are described by *Sattler, 1999*. In his work, as an example, the results of generation are given for different domains of models DMI-HIRLAM – G, N, E, and D. All available classes from the Global Ecosystems Legend were reclassified into 20 classes, which are similar to the Biosphere Atmosphere Transfer Scheme Legend (*Dickinson et al., 1986; 1993*), except classes called - forest/fields and fields/woods. In each grid cell any class of 20 is represented by fraction of area covered within the cell.

The briefly summarized generation procedure with omitted number of steps (given by *Sattler, 1999; Sattler, 2000*) is shown in Fig. 3.1.1. Note, in preprocessing two types of files are used/created: HDF and GRIB-formats. The second is used as input by models; the first is used for processing, visualization and check of obtained fields for consistency.

As seen, on a first step/run, original available datasets of different resolution and quality are reprocessed into intermediate datasets having requested number of parameters and reevaluated/regrouped land use classes. Then, depending on sizes and resolution of the new selected modelling domain, the climate generation files (in total 12 – one file for each month) for the same number of classes are produced. Note, the current version of ISBA LSS of HIRLAM uses approach of 5 major tiles (water, ice, no vegetation, low vegetation, and forest); and therefore, the climate generation files are reprocessed again using the first dominating and secondary class approach to fit ISBA request. This is shown (Fig. 3.1.1) on example of reclassification of original 94 into 20 land use classes with the following reduction to 5 major tiles of LSS. Each tile contains a set of land use classes (see *Bringfelt, 1996*; *Sattler, 1999;* and DMI-HIRLAM ISBA scheme): water – 2, ice – 2

classes, no vegetation – 2, low vegetation – 9, and forest – 5. Note, each monthly output file contains records for the landmask, height, albedo, soil type, moisture, sea surface temperature, deep soil temperature, roughness, first and secondary dominating land use classes, etc. Although some of the parameters are calculated for each grid cell of the domain, the averaged roughness, leaf area index, albedo, etc. are used from the hard-coded tables of the INI_VEG.f subroutine.

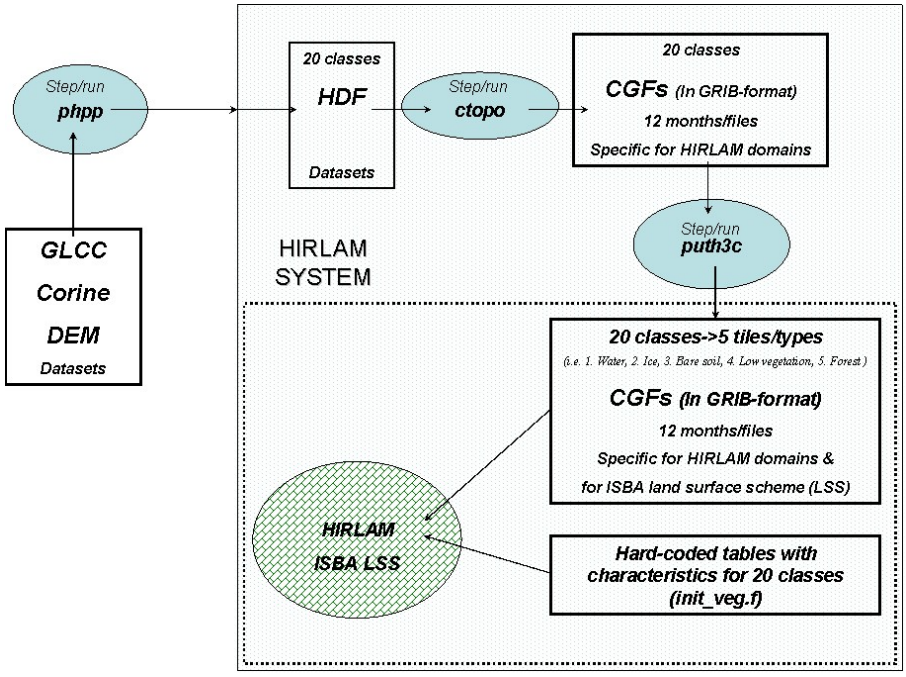

Fig. 3.1.1. General scheme of climate generation files production for the DMI-HIRLAM system.

A set of physiographical and climatic parameters is included into the GRIB-files. As shown in Appendix 4, in order to access/read these parameters the ID numbers (ID) from the list (see "Description" column) in columns: "Parameter", "LevelType", and "Level" should be selected. For example, in order to read information on parameter called "fraction of low vegetation", the IDs - for "Parameter" is equal to **81**, "LevelType" - **105**, and "Level" - **904** - all these must be specified.

3.2. Classification for the U01 Modelling Domain

For the U01 domain, as shown in Fig. 3.2.1a, the 1st dominating class for the 3 ISBA tiles (of 5 major) – water, low vegetation, and forest tiles - consist of 55.41% (class 15 - sea), 27.25% (class 1 - cropland), and 15.19% (class 3 – evergreen forest) of the grid cells (in total 97.85%), respectively. Except 3 mentioned classes, other classes (in total another 7) dominate only in 2.75% of the grid cells of the U01 modelling domain. Hence, other 10 of 20 classes are not represented at all as the 1st dominating class. For the secondary dominating class, it should be noted (as shown in Fig. 3.2.1b) that there is not at all such dominating class in 81.83% of the cells. The rest (18.17%) is redistributed in the following manner: 8.43% of cells showed that the 2nd dominating class is class #1 from the low vegetation tile; 2.27% - class #3 from the forest tile; and 1.82% - class #15 from water tile. Excluding these 3 most common classes, another 10 classes contribute in total 5.65%. I.e. in total only 13 classes (out of 20) are represented in the U01 modelling domain.

Examples of visualized outputs of climate generation files/fields are shown in Figs. 3.2.2-3.2.3 for the U01 modelling domain for the month of January. Geographical distribution of fractions for the water tile is shown in Fig. 3.2.2a, low vegetation tile - Fig. 3.2.2b, and forest tile - Fig. 3.2.2c. As seen the classes of the low vegetation tile are more represented over the Danish territories and the south of Sweden compared with classes of the forest tile. The land use classes (out of

20) for each tile are shown in Figs. 3.2.3. As seen, both classes – cropland as class 1 (Fig. 3.2.3b) for low vegetation tile and evergreen forest class 3 (Fig. 3.2.3c) for forest tile - dominate compared with others. In Fig. 3.2.3a the class 14 represented by flag of is the inland water, and class 15 represented by flag of the sea water.

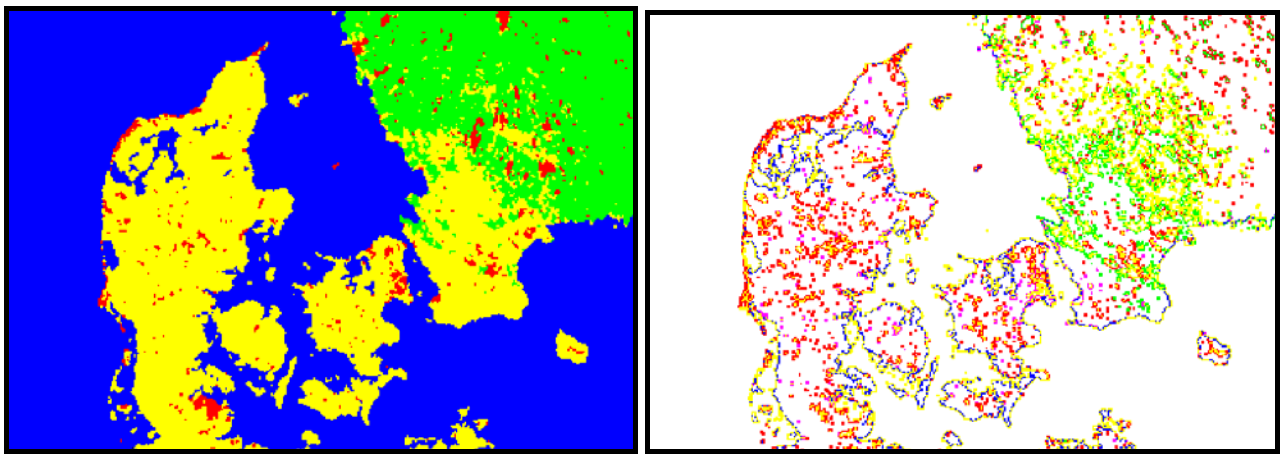

(a) (b)

Fig. 3.2.1. Distribution of the a) first dominating class and b) second dominating class within major tiles represented in the U01 domain and generated for the HIRLAM ISBA LSS use. Used colors: blue – water tile (class 15 - sea); green – forest tile (class 3 – evergreen forest); yellow – low vegetation tile (class 1 - cropland), red – all other classes; white – no second dominating class.

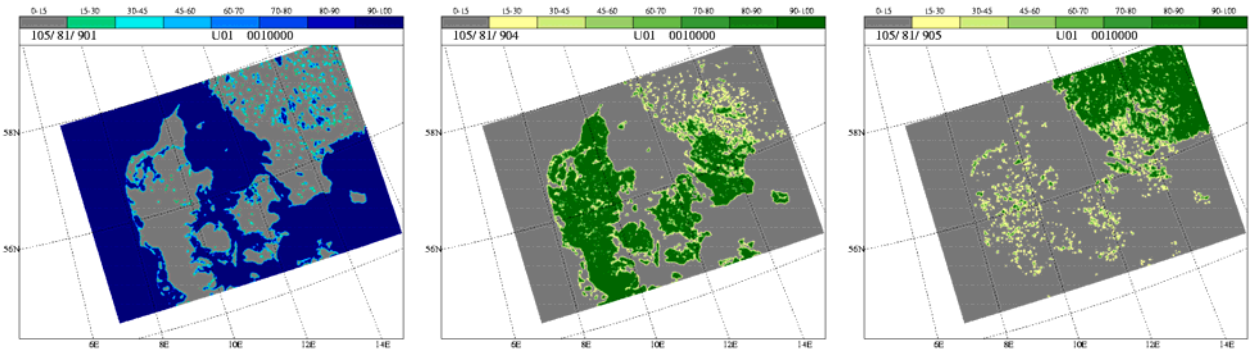

(a) (b) (c)

Fig. 3.2.2. Example of output of climate generation file for January: fractions (in percentage) of three (from 5) major tiles – a) water, b) low vegetation and c) forest - represented in the U01 domain and generated for the HIRLAM ISBA LSS use.

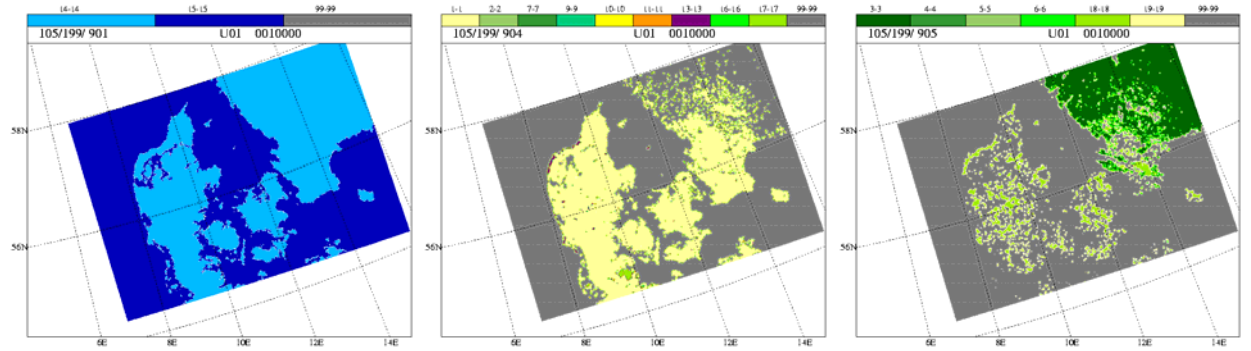

(a) (b) (c)

Fig. 3.2.3. Example of output of climate generation file for January: types of classes (from 20) for three (from 5) major tiles - a) water, b) low vegetation, and c) forest - represented in U01 domain and generated for the HIRLAM ISBA LSS use.

3.3. Classification for the I01 Modelling Domain

Another example of land use classification is given for the land surface scheme of the SM2_U module for the DMI-HIRLAM-I01 modelling domain used in the FUMAPEX project activities (*Mahura et al., 2005d; Mahura et al., 2005e; Mahura et al., 2005f*). Its scheme is composed of 7 major formulations/tiles. Since this module is used for urban modeling purposes, the higher resolution and quality datasets are crucial input data. Hence, the classification of the high resolution CORINE dataset was done on the selected domain located between 10.442-13.413ºE and 54.814-56.499ºN (Fig. 2.1b) with a resolution of 0.014 degrees. For simplicity, since the CORINE Swedish data were not available these were excluded from further analysis. The results of the land-use classification and its statistics are shown in Tab. 3.3.1 and Fig. 3.3.1-3.3.2.

The re-classification of the CORINE Land Cover Legend into 7 major types/tiles (used by the LSS of the Sub-Meso Soil Model Urbanized version, SM2_U) is given in Appendix 3. Note, that original legend has references/records to classes' titles in English, German, and French languages (only English was kept for simplicity). This classification is represented by 7 types of surfaces of – vegetation on natural (*vegn*), natural (*nat*), vegetation on artificial (*vega*), artificial (*art*), bare (*bare*), buildings (*bat*), and water (*eau*). For each type the exact number was given such as 101-107 (see at the end of Appendix 3). Then, the list of classes (ranging from 1 to 100) was reclassified, and each class was assigned to one of the seven types. Note, "ignore" was assigned to classes which were not presented in the CORINE vs. GLCC datasets, but still needed for climate generation procedure.

Tab. 3.3.1. Distribution of surface types and its characteristics in the I01 modeling domain based on classification of the CORINE dataset.

Characteristic Surface type	PTS	DTS
vegn	12.74	2.74 (401)
vega	**1.48**	**0.08 (12)**
nat	12.07	1.83 (268)
art	**0.54**	**0.12 (18)**
bare	29.78	21.79 (3189)
bat	9.54	2.25 (329)
eau	75.49	70.74 (8279)

Tab. 3.3.1 shows the percentage of the grid cells in the modeling domain where a class is represented, and the percentage of the gird cells where a class is dominated compared with others. The PTS (represented type of surface) is the percentage of cells from the total number of cells in domain where, at least, a fraction of surface type is presented. The DTS (dominated type of surface) is percentage of cells from total number of cells in domain where a fraction of selected surface type is the highest compared with other types; values given in brackets are number of cells with this type in the modeling domain.

As seen in Fig. 3.3.1bc, the artificial surfaces (*art*) and vegetation on artificial surfaces (*vega*) classes are presented mostly in the Copenhagen metropolitan area. These two including *bat* (Fig. 3.3.1a) are related to urbanized areas. The water (*eau*) and bare (*bare*), as shown in Fig. 3.3.2a, types of surfaces have the highest representations in this modelling domain, and these dominate in more than 90% of the grid cells. Two other types – *nat* and *vegn* – shown in Fig. 3.3.2bc, are also well shown in the domain; and although these types presented in 24.81% of the cells, they dominate only in 4.57% of the cells.

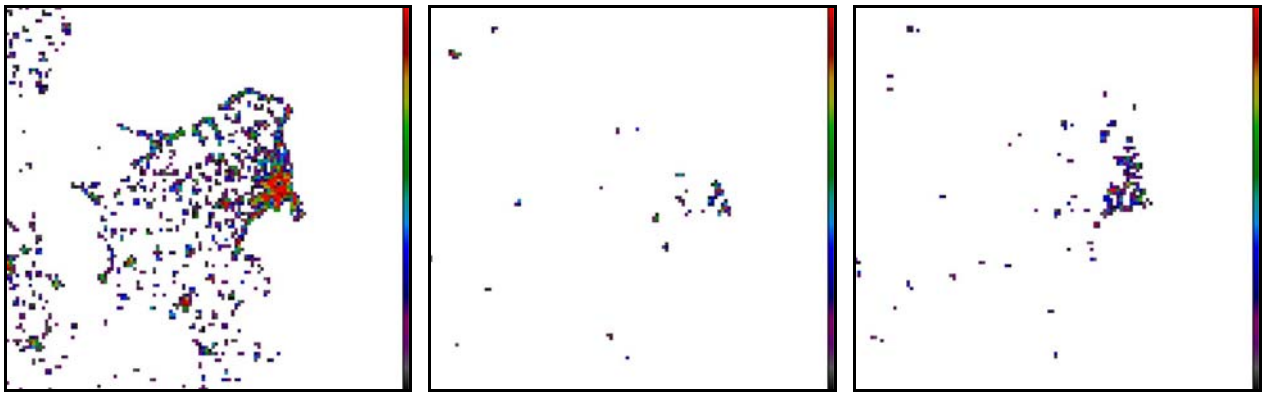

(a) (b) (c)

Fig. 3.3.1. Distribution of fractions for surface types - (a) bat, (b) art and (c) vega - in grid cells of model domain (scale on the right side is percentage/fraction of type in grid cell : 0.01 - at bottom, 1 – at top of the scale).

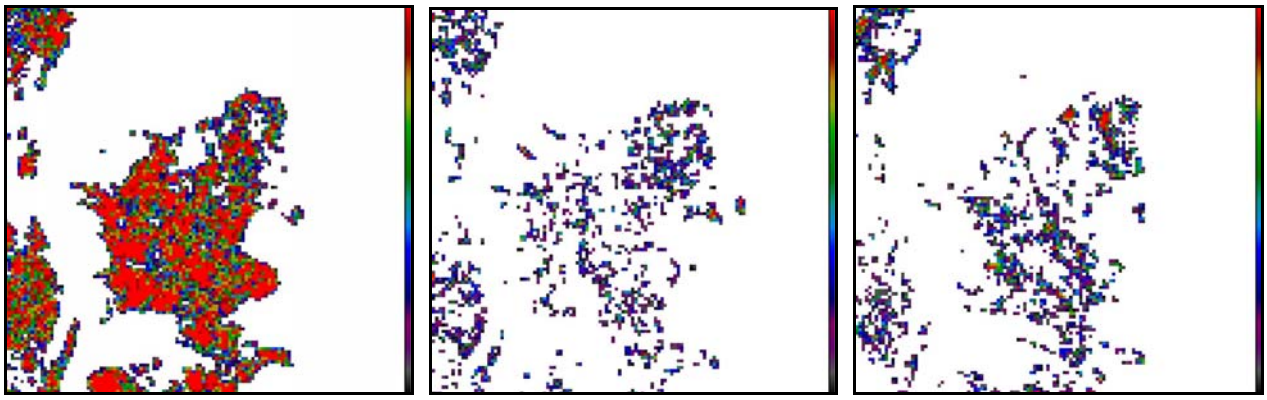

(a) (b) (c)

Fig.3.3.2. Distribution of fractions for surface types - (a) bare, (b) nat and (c) vegn - in grid cells of model domain (scale on the right side is percentage/fraction of class in grid cell : 0.01 - at bottom, 1 – at top of the scale).

4. DMI-HIRLAM-U01 Model Specific Cases and Long-Term Simulations

The DMI-HIRLAM model components include the digital filtering initialization, semi-Lagrangian advection scheme, and a set of physical parameterizations such as the Savijaervi radiation, STRACO condensation, CBR turbulence and ISBA schemes (*Undén et al., 2002; Sass et al., 2002*).

Originally, the runs were performed daily during spring-summer of 2005. Then, from these runs several specific cases/dates were selected for analysis.

First, the ISBA land surface scheme performance was evaluated for modified roughness, albedo, and added anthropogenic fluxes over the urban grid cells of modelling domain. The major focus was on the Copenhagen, Denmark and Malmö, Sweden metropolitan areas.

Second, a typical date with surface winds of 5-10 m/s and dominating atmospheric transport by westerlies was selected to test the performance of the DMI-HIRLAM-S05 vs. U01 models.

Third, a date with the low winds over the Island of Zeeland and surroundings was analyzed. To select such dates the ground observation and radiosounding data from the Danish stations were routinely analysed. For low winds conditions the following criteria were selected: 1) wind velocities of less than 5 m/s in low levels, 2) wind directions from the south-east sector of the Island of Zeeland, 3) winds of similar directions and magnitudes on radiosounding diagrams. This date was also used to test performance of the DMI-HIRLAM-S05 vs. U01 models.

In addition, analysis of dates during January 2004 - June 2005 showed that there are several specific dates/periods (7 in 2004 and 7 in 2005) with 10 m wind speeds of less than 5 m/s over the Copenhagen metropolitan area and surroundings, and these might be also useful, depending on tasks, in other specific case studies:

- 25-26 January 2004,
- 5-6 and 30 March 2004,
- 26 April 2004,
- 5 and 17-18 June 2004,
- 3-4 September 2004,
- 25 and 30-31 March 2005,
- 1-2 April 2005,
- 22, 27, and 30 May 2005,
- 19 June 2005.

Note, on average, for a diurnal cycle (00-24 UTC) forecast, each DMI-HIRLAM run for the U01 domain required 4.2 hours of CPU time (for 1 processor on DMI NEC-SX6 machine), and the memory used is 5.3 Gb. The boundary conditions of the DMI-HIRLAM-S05 model were applied. The climate generation files prepared for U01 domain were used. The total space occupied by output files used further for analysis is about 450 Mb.

In addition, the simulations are performed also for a two month period of July-August 2004 for the same domain. At the first step, the T15 and S05 versions of DMI-HIRLAM were re-run. Then, the boundary conditions files for the U01 model were re-calculated and simulations will be re-done for a diurnal cycle on the U01 domain. Finally, this U01 output will be also compared with S05.

Finally, several tests of sensitivity of the ISBA scheme of the DMI-HIRLAM high resolution modelling to modifications in parameters of roughness, albedo, and contribution of anthropogenic flux were done by *Mahura et al., 2005a; Baklanov et al., 2005* for the typical date and for urbanized areas of Copenhagen and Malmö. Analysis of the land surface scheme sensitivity for these parameters for a specific date with the low wind conditions is summarized by *Mahura et al., 2005a, Mahura et al., 2005b* for the Copenhagen metropolitan area. Moreover, due to modifications of the ISBA scheme the estimation of temporal and spatial variability of simulated concentration and deposition fields (calculated by the Local Scale Model Chain of ARGOS system) resulted from hypothetical accidental release of radioactivity in the Copenhagen metropolitan area are underway (*Mahura et al., 2005c*). In this analysis several specific case studies – low winds, typical situation, high precipitation, and high winds dates during – will be evaluated.

4.1. Typical Date Case Study for DMI-HIRLAM High Resolution Runs

During period studied, the date of 1 Jun 2005 was characterized by "typical" western wind conditions over the Island of Zeeland in the modelling domain. The sounding diagrams of the Jegersborg (55.76ºN and 12.53ºE) station on 1 June showed inversions around 800 and 700 hPa levels with western winds of up to 10 m/s. At 12 UTC on the same day, the diagram underlined that the western winds persisted, and almost isothermal layer between 850-800 hPa was observed. On 2 June 2005 at 00 UTC, the wind velocities decreased in the boundary layer, the short inversion was observed near the surface and a wide inversion layer - above 800 hPa level.

For this date a comparative analysis between simulation outputs of the DMI-HIRLAM-S05 vs. U01 models was performed for the wind at 10 meters and temperature at 2 meters. The diurnal cycle was evaluated by considering minimum, maximum and average difference between two models outputs at exact UTC standard terms. The wind and temperature (2D fields) for both models over the U01 modelling domain, as examples, at 12 and 21 UTC terms of 1 June 2005 are given in Appendix 5, and summary is given in Tabs. 4.1.1 and 4.1.2. The difference plots (by subtracting

outputs of the DMI-HIRLAM-S05 vs. U01 models at grid cells of the U01 modelling domain) between these two models of different resolutions are shown for the wind and temperature in Figs. 4.1.1 and 4.1.2, respectively.

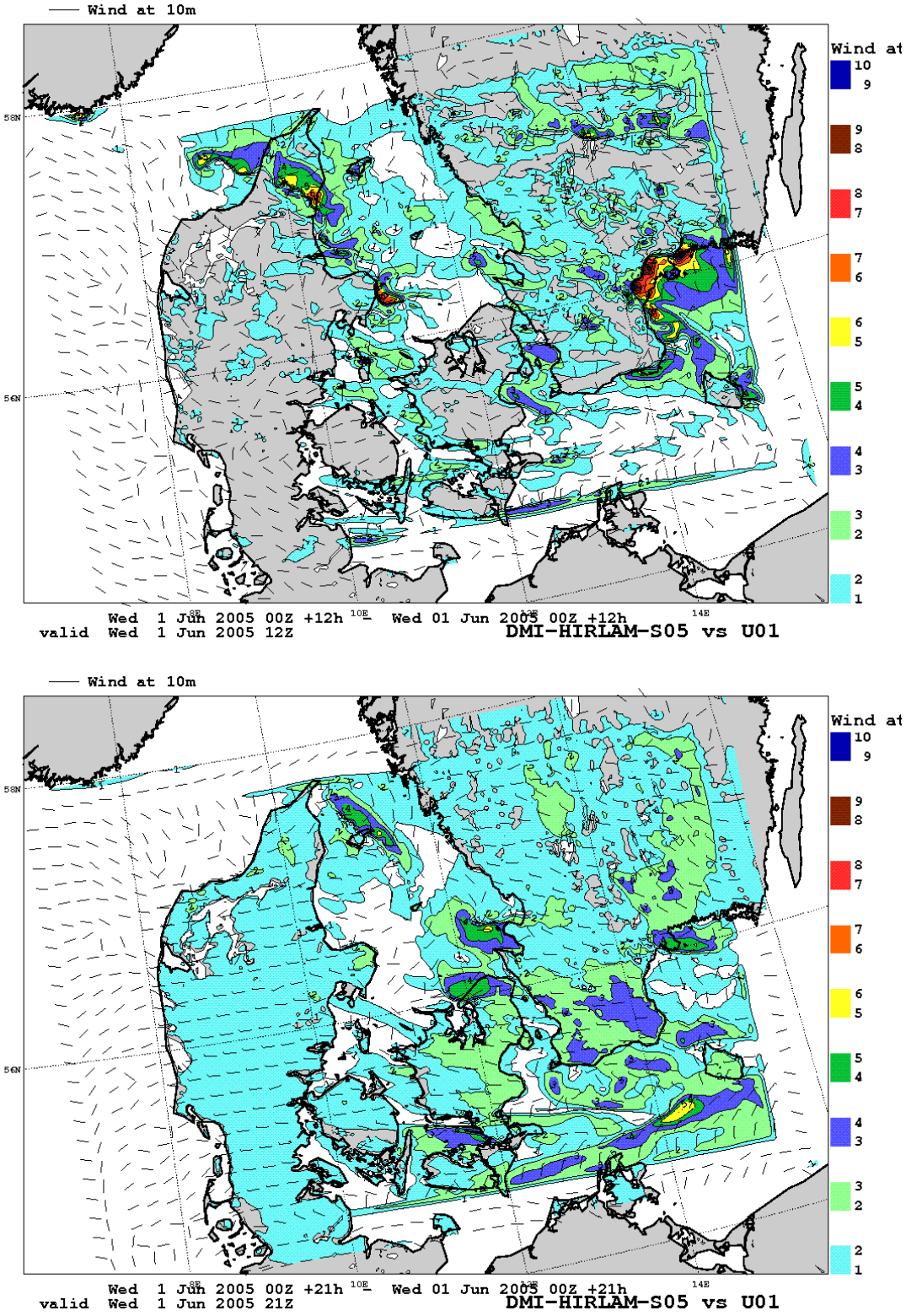

Fig. 4.1.1. Difference plots for the wind fields at 10 m over the U01 modelling domain simulated by the DMI-HIRLAM-S05 vs. U01 models at terms of (top) 12 UTC and (bottom) 21 UTC on 1 June 2005.

As seen in Tab. 4.1.1, in the modelling domain, on a diurnal cycle, the averaged wind velocity

varied from 4 (4.4) to 6 (6.5) m/s for the U01 (S05) models outputs. The maximum simulated wind velocity was 14.5 (14.1) m/s for U01 (S05) and it was observed at 00 UTC. On average, the difference (for each of given in Tab. 4.1.1 UTC term as $\mathbf{U}_{S05}-\mathbf{U}_{U01}$) in simulated wind velocities between the U01 and S05 models was less than 0.2 m/s, where during 06-15 UTCs the U01 model showed slightly higher wind velocities compared with S05. In other parts of the day, the U01 produced slightly lower velocities.

Model	**U01**		**S05**		**DIF - S05 vs. U01**	
Characteristic	**avg**	**max**	**avg**	**max**	**avg**	**max**
UTC term						
0	6.04	14.47	6.52	14.11	0.74	3.05
3	5.71	12.58	6.12	11.88	1.08	4.64
6	5.57	12.24	5.49	11.41	0.73	5.75
9	5.63	12.99	5.60	10.83	0.77	6.99
12	6.02	10.82	5.92	10.32	1.01	9.90
15	5.84	11.25	5.79	10.28	1.12	7.82
18	5.27	11.08	5.38	9.97	1.07	8.73
21	4.20	10.87	4.72	8.86	1.19	6.00
24	4.00	10.53	4.36	8.86	1.06	5.58
Daily avg	**5.36**	**11.87**	**5.54**	**10.72**	**0.97**	**6.50**

Tab. 4.1.1. Summary table for the wind velocities at 10 m over the U01 modelling domain simulated by the DMI-HIRLAM-S05 vs. U01 models at UTC terms on 1 June 2005.

But, analysis of the wind velocity difference plots (examples are presented in Fig. 4.1.1) at each UTC term (as shown in Tab. 4.1.1 for **DIF - S05 vs. U01)** for the wind velocity showed that the average difference is about 1 m/s with higher winds simulated by the DMI-HIRLAM-S05 model. Note, over particular geographical locations, as shown in Appendix 5 and Fig. 4.1.1, this difference may be maximum up to several meters per second. This depends also on how the higher resolution model resolve the smaller scale eddies as well as the simulated temperature over domain.

Model	**U01**			**S05**			**DIF - S05 vs. U01**		
Characteristic	**min**	**avg**	**max**	**min**	**avg**	**max**	**min**	**avg**	**max**
UTC term									
0	6.17	10.88	13.63	6.22	10.02	12.76	–4.63	–0.86	1.59
3	3.92	9.46	12.17	5.10	9.66	12.42	–3.07	0.21	3.25
6	7.30	10.38	12.86	6.49	10.03	12.52	–4.08	–0.35	1.97
9	8.67	11.88	16.11	8.79	11.04	13.12	–4.26	–0.84	1.25
12	9.19	12.65	18.29	9.62	11.68	14.72	–4.65	–0.98	1.94
15	9.59	12.76	17.53	9.72	11.93	14.96	–5.02	–0.83	3.00
18	9.00	12.05	15.43	9.58	11.72	14.02	–3.16	–0.33	2.83
21	6.75	10.29	13.95	8.36	10.71	13.14	–2.07	0.42	3.96
24	4.39	9.23	13.52	6.36	9.87	12.72	–2.26	0.63	4.99
Daily avg	**7.22**	**11.06**	**14.83**	**7.80**	**10.74**	**13.38**	**–3.69**	**–0.33**	**2.75**

Tab. 4.1.2. Summary table for the temperature at 2 m over the U01 modelling domain simulated by the DMI-HIRLAM-S05 vs. U01 models at UTC terms on 1 June 2005.

As seen in Tab. 4.1.2, in the modelling domain, on a diurnal cycle, the averaged temperature varied from 9.2 (9.7) to 12.8 (11.9) ºC for the U01 (S05) models outputs. The maximum temperature was 18.3 (15) ºC for U01 (S05) and it was observed at 12 (15) UTC. The minimum temperature was 3.9 (5.1) ºC for U01 (S05) and it was observed at 03 UTC. On average, the difference (for each of given in Tab. 4.1.2 UTC term as $\mathbf{T}_{S05}-\mathbf{T}_{U01}$) in simulated temperatures between the U01 and S05 models was less than 0.3ºC. For maximum this difference was about 1.5ºC (U01 predicted higher maximum compared with S05), and for minimum it was 0.6ºC.

But, analysis of the wind velocity difference plots (examples are presented in Fig. 4.1.2) at each UTC term (as shown in Tab. 4.1.2 for **DIF - S05 vs. U01)** for the temperature showed that the average difference is also about 0.3 ºC, but the U01 model temperature output has higher diurnal variability of difference ranging from –4.7 to +5ºC.

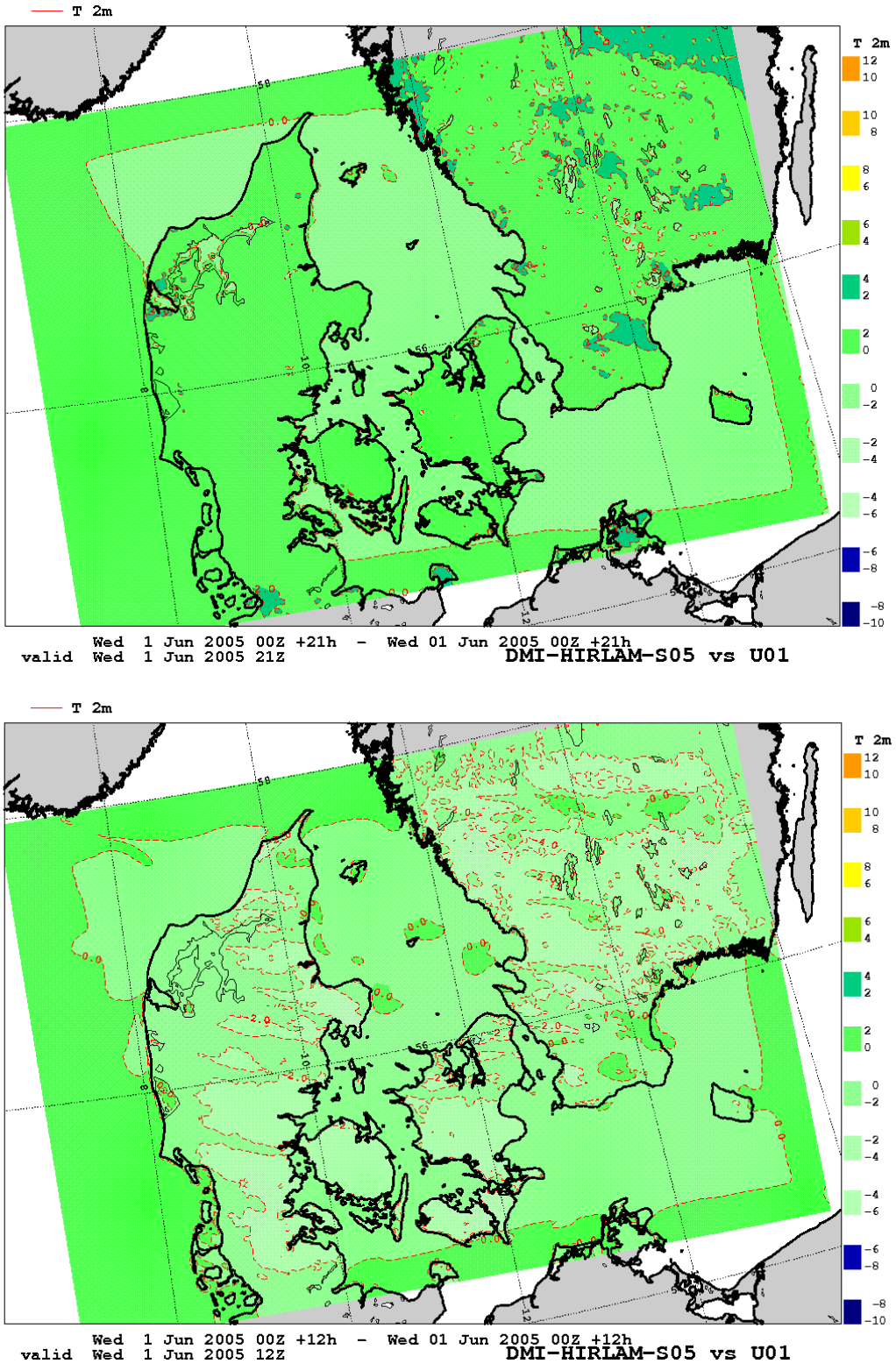

Fig. 4.1.2. Difference plots for the temperature fields at 2 m over the U01 modelling domain simulated by the DMI-HIRLAM-S05 vs. U01 models at terms of (top) 12 UTC and (bottom) 21 UTC on 1 June 2005.

4.2. Low Winds Case Study for DMI-HIRLAM High Resolution Runs

During period studied, the date of 22 May 2005 was characterized by low winds conditions over the Island of Zeeland in the modelling domain. The sounding diagrams of the Jægersborg station (55.76ºN, 12.53ºE) on 22 and 23 May 2005, 00 UTC showed the presence of inversion in the lowest layers and isothermal layer around 700 hPa level. At 12 UTC, the inversion and isothermal layers disappeared. During the day, the low velocities of winds from the southeastern-southwestern sector from the station were observed within the atmospheric boundary layer up to 850 hPa.

For this date a comparative analysis between simulation outputs of the DMI-HIRLAM-S05 vs. U01 models was performed for the wind at 10 meter and temperature at 2 meter. The diurnal cycle was evaluated by considering minimum, maximum and average difference between two models outputs at exact UTC standard terms. The wind and temperature (2D fields) for both models over the U01 modelling domain, as examples, at 12 and 21 UTC terms on 22 May 2005 are given in Appendix 6, and summary is given in Tabs. 4.2.1 and 4.2.1. The difference plots (by subtracting outputs of the DMI-HIRLAM-S05 vs. U01 models at grid cells of the U01 modelling domain) between these two models of different resolutions are shown for the wind and temperature in Figs. 4.2.1 and 4.2.2, respectively.

Model	**U01**		**S05**		**DIF - S05 vs. U01**	
Characteristic	**avg**	**max**	**avg**	**max**	**avg**	**max**
UTC term						
0	2.92	7.87	3.38	8.13	0.73	3.82
3	3.60	8.21	3.67	8.76	0.92	6.16
6	3.69	9.17	3.63	10.14	0.86	5.74
9	3.61	8.19	3.35	8.73	0.79	7.09
12	4.15	8.52	3.74	8.09	1.03	8.35
15	4.25	9.91	3.78	8.83	1.16	10.75
18	4.04	9.39	3.74	8.19	0.97	7.52
21	3.30	9.75	3.23	8.06	0.83	7.97
24	3.11	8.51	3.09	6.88	0.93	7.36
Daily avg	**3.63**	**8.84**	**3.51**	**8.42**	**0.91**	**7.20**

Tab. 4.2.1. Summary table for the wind velocities at 10 m over the U01 modelling domain simulated by the DMI-HIRLAM-S05 vs. U01 models at UTC terms on 22 May 2005.

As seen in Table 4.2.1, in the modelling domain, on a diurnal cycle, the averaged wind velocity varied from 2.9 (3.1) to 4.3 (3.8) m/s for the U01 (S05) models outputs. The maximum simulated wind velocity was 9.9 (10.1) m/s for U01 (S05) and it was observed at 15 (06) UTC. On average, the difference (for each of given in Tab. 4.2.1 UTC term as $\mathbf{U}_{S05}$–$\mathbf{U}_{U01}$) in simulated wind velocities between the U01 and S05 models was less than 0.5 m/s, where at the beginning of simulation (during the first several hours) the S05 model resulted in slightly higher winds (and during the first half of the day – in higher maximum wind velocities too) compared with the rest of the day, when the U01 model showed slightly higher wind velocities.

But, analysis of difference plots at each UTC term (as shown in Tab. 4.2.1 for **DIF - S05 vs. U01)** for the wind velocity showed that the average difference is about 1 m/s with higher winds simulated by the DMI-HIRLAM-S05 model. Although, it should be noted that over particular geographical locations, as shown in Appendix 6 and Fig. 4.2.1, this difference may be up to several meters per second.

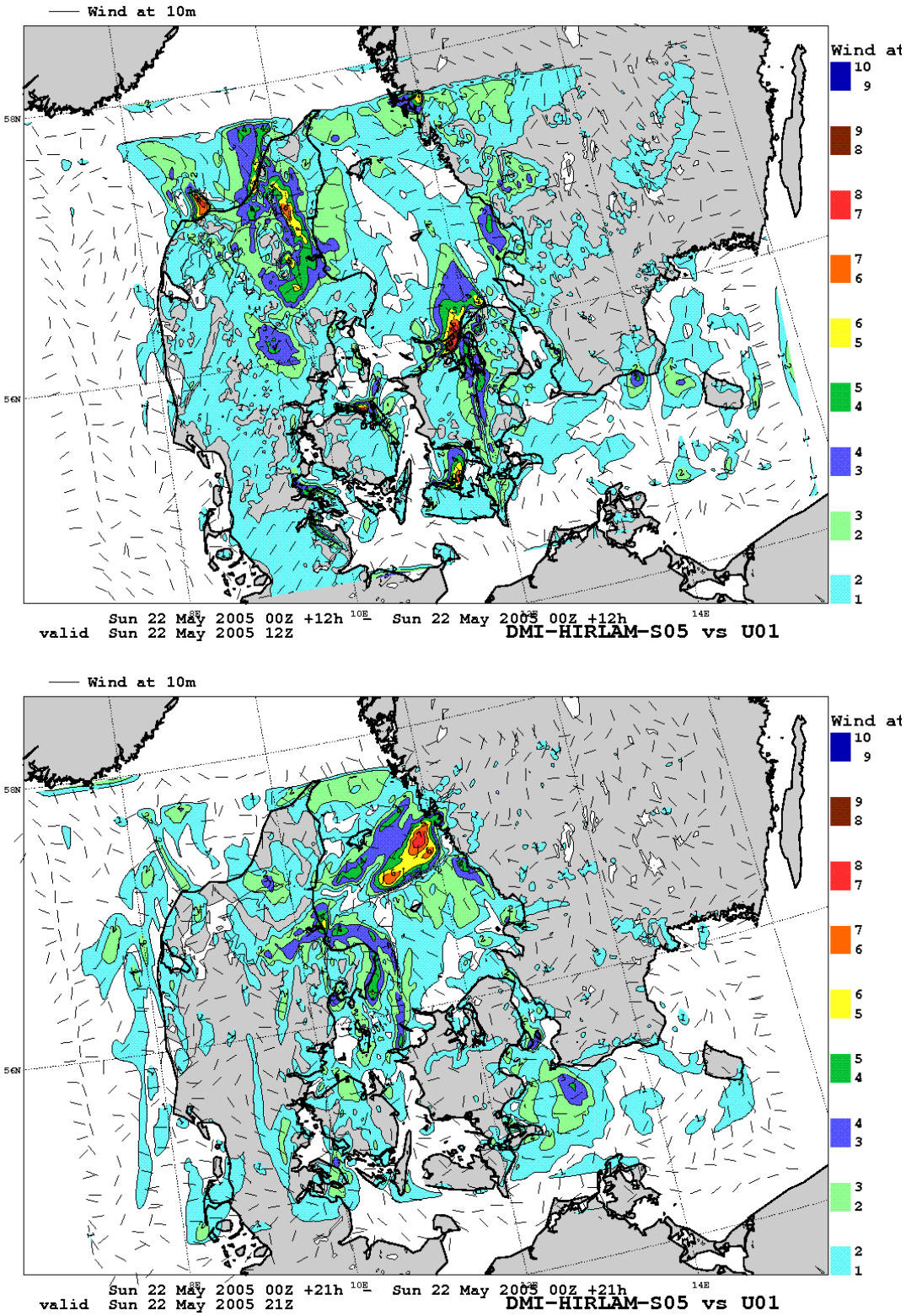

Fig. 4.2.1. Difference plots for the wind fields at 10 m over the U01 modelling domain simulated by the DMI-HIRLAM-S05 vs. U01 models at terms of (top) 12 UTC and (bottom) 21 UTC on 22 May 2005.

As seen in Tab. 4.2.2, in the modelling domain, on a diurnal cycle, the averaged temperature varied from 9 (9.7) to 13.2 (10.5) ºC for the U01 (S05) models outputs. The maximum temperature was 23.7 (14.7) ºC for U01 (S05) and it was observed at 12 (15) UTC. The minimum temperature was 4.3 (6.5) ºC for U01 (S05) and it was observed at 21 UTC. On average, the difference (for each

of given in Tab. 4.2.2 UTC term as $\mathbf{T}_{S05}-\mathbf{T}_{U01}$) in simulated temperatures between the U01 and S05 models was less than 0.9ºC. For maximum this difference was about 4.1ºC (U01 predicted higher maximum compared with S05), and for minimum it was 1.2ºC.

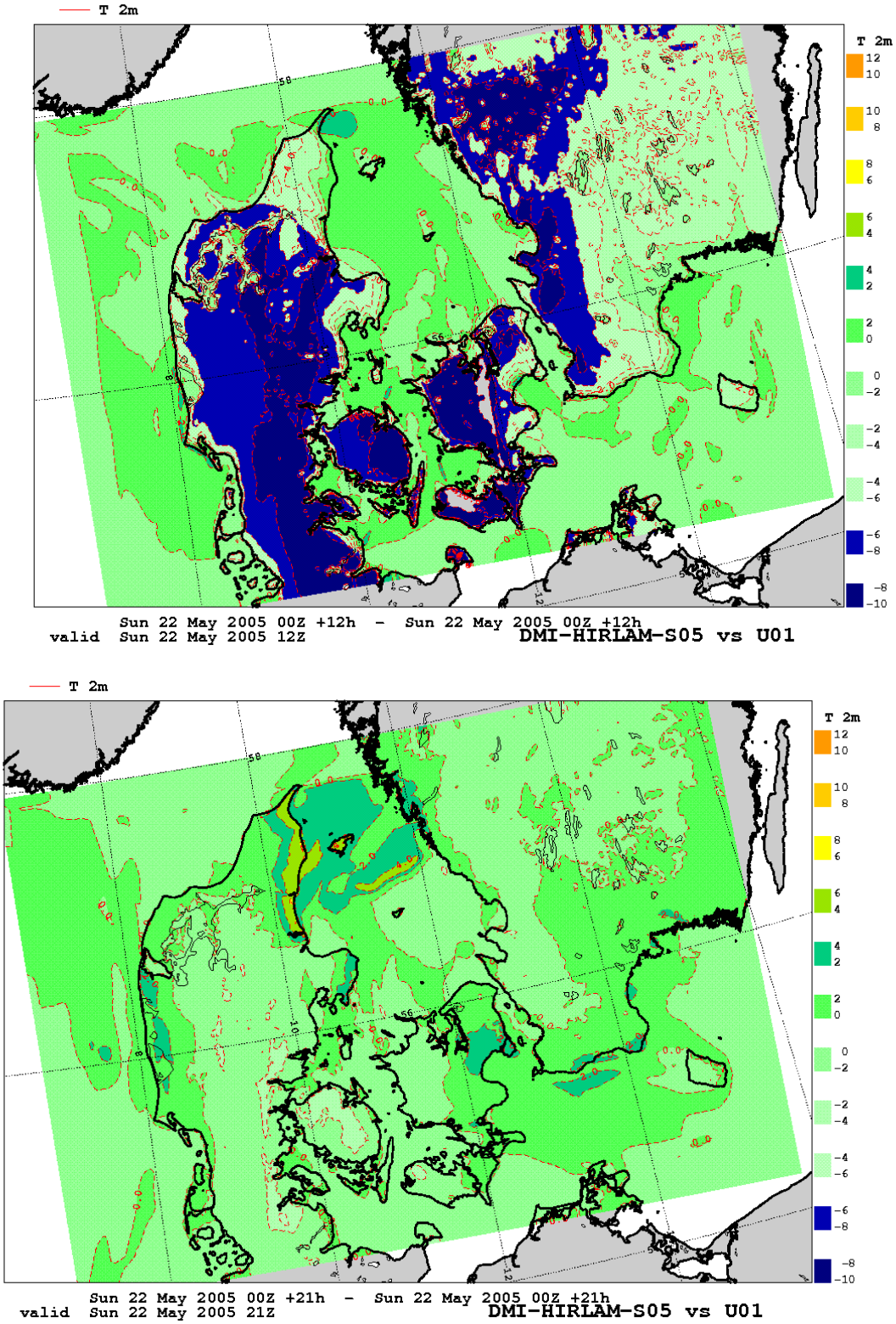

Fig. 4.2.2. Difference plots for the temperature fields at 2 m over the U01 modelling domain simulated by the DMI-HIRLAM-S05 vs. U01 models at terms of (top) 12 UTC and (bottom) 21 UTC on 22 May 2005.

But, analysis of the wind velocity difference plots (examples are presented in Fig. 4.2.2) at

each UTC term (as shown in Tab. 4.2.2 for **DIF - S05 vs. U01)** for the temperature showed that the daily average difference is also about 0.9 ºC, but the U01 model temperature output has higher diurnal variability of difference ranging from –6.8 to +4.2ºC (with even higher differences at particular terms as shown in Tab. 4.2.2). Note, the temperature differences in models became even more visible when the typical vs. low wind conditions are compared.

Model	U01			S05			DIF - S05 vs. U01		
Characteristic	min	avg	max	min	avg	max	min	avg	max
UTC term									
0	6.88	9.93	12.40	6.82	9.79	12.50	–3.17	–0.14	2.08
3	4.52	8.98	11.74	6.73	9.71	12.64	–2.02	0.73	5.01
6	6.72	9.98	14.96	6.91	9.89	13.07	–5.01	–0.09	2.68
9	6.32	11.75	21.04	7.06	10.17	13.96	–9.87	–1.58	3.12
12	5.91	13.02	23.66	7.02	10.39	14.28	–11.39	–2.63	3.87
15	5.90	13.19	23.42	6.98	10.47	14.73	–11.58	–2.72	3.63
18	4.93	12.27	21.65	6.63	10.41	13.91	–9.93	–1.86	5.02
21	4.26	10.02	16.39	6.45	10.03	13.40	–4.23	0.00	6.47
24	5.12	9.36	13.37	6.68	9.84	13.33	–3.60	0.48	5.38
Daily avg	**5.62**	**10.94**	**17.63**	**6.81**	**10.08**	**13.54**	**–6.76**	**–0.87**	**4.14**

Tab. 4.2.2. Summary table for the temperature at 2 m over the U01 modelling domain simulated by the DMI-HIRLAM-S05 vs. U01 models at UTC terms on 22 May 2005.

4.3. Land Surface Scheme Sensitivity for DMI-HIRLAM High Resolution Runs

Several specific cases/dates during spring of 2005 were studied employing the DMI-HIRLAM-U01 model. I.e. dates, when the dominating atmospheric transport over the Zeeland from the south-east sector was observed with low winds conditions, were studied. In these runs in the ISBA scheme (*Rodriguez et al., 2003; Navascues et al., 2003*) of HIRLAM, first, the roughness for cells, where the urban class is presented in the modeling domain, was increased up to 1 m and 2 m. Second, the albedo was increased. Third, the contribution of anthropogenic flux ranging from 10 to 200 W/m^2 was incorporated into the land surface scheme. Here, as an example of such a case – DMI-HIRLAM run for 30 March 2005, 00 UTC + 24 hour forecast – is analyzed.

The meteorological fields' simulations for the metropolitan areas were driven using the DMI-HIRLAM-S05 model (resolution of 5 km) boundary conditions. These conditions were used as input for simulation of meteorological fields for the DMI-HIRLAM-U01 research version (resolution of 1.4 km) which includes the Copenhagen (CPH) and Malmö (MAL) metropolitan areas and surroundings. Note, for each specific date 8 independent runs were performed: 1 control (no modifications in ISBA scheme) DMI-HIRLAM operational run; and modified 4 - for anthropogenic fluxes, 2 – for roughness, and 1 – for albedo.

The diurnal cycle of meteorological variables such as wind velocity (at 10 m) and temperature (at 2 m) in the low surface layer of atmosphere as well as sensible and latent heat fluxes were analyzed comparing outputs of the DMI-HIRLAM control run vs. runs with modified parameters for urban class. At each UTC term, the 2D (values in latitude vs. longitude gridded modeling domain) difference fields for mentioned variables were produced/analyzed by subtracting outputs from the original standard DMI-HIRLAM operational run without any changes made and from the same run with changes made for roughness, albedo, and anthropogenic flux.

Roughness

As seen in Fig. 4.3.1, the increased roughness in urbanized areas (suburbs of the Copenhagen

(Denmark) and Malmö (Sweden)) changed the structure of the surface wind field. In particular, during the day time the wind velocity over these urban areas is lower by 1-3 m/s. The increase of roughness up to 2 m decrease velocities by 1-4 m/s and areas, where this effect is visible, became larger and more pronounced not only near CPH and MAL, but also for other less urbanized cities. During the night this effect is smaller (as shown in Tab. 4.3.1).

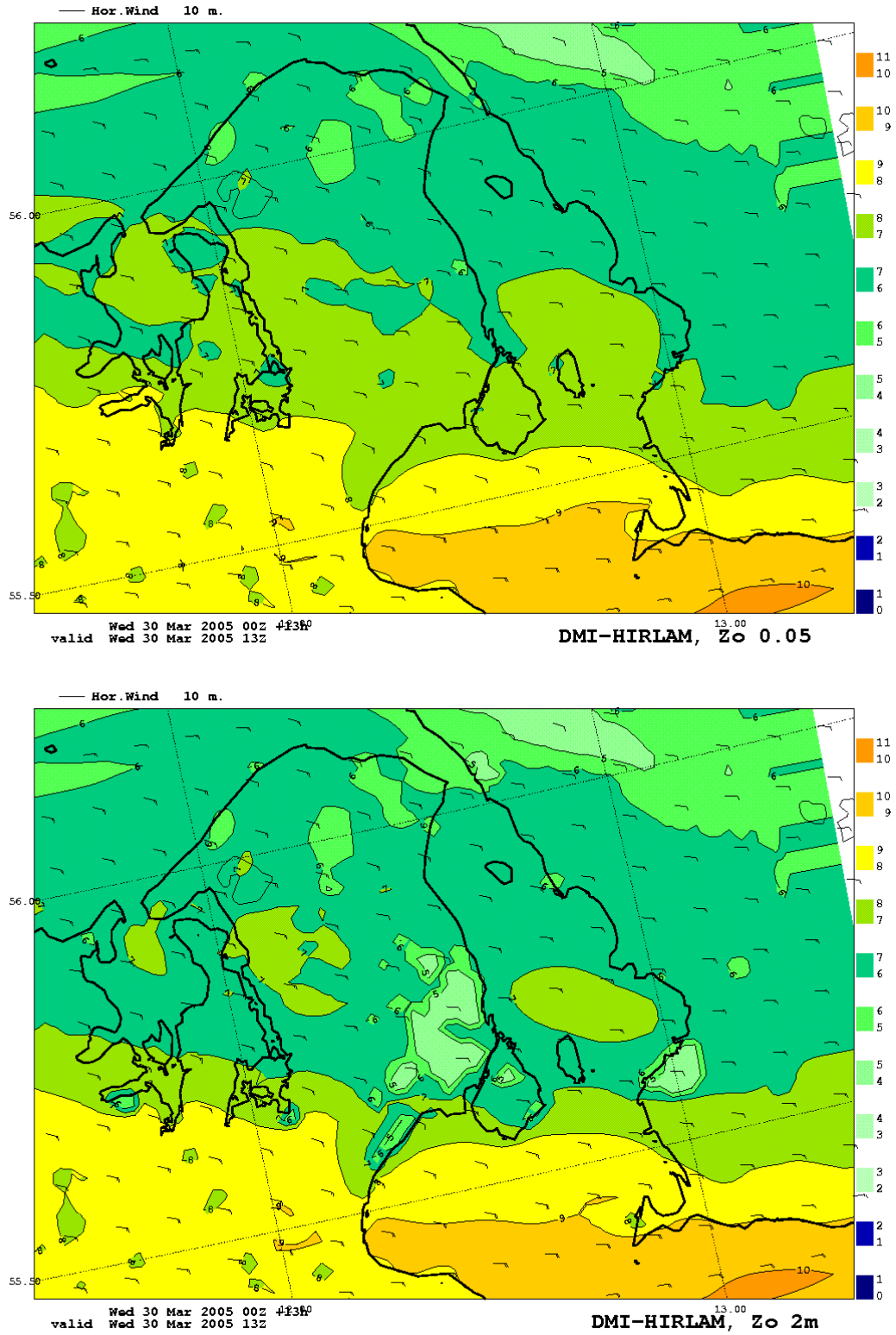

Fig. 4.3.1. Simulated wind field at 10 m for roughness of 0.05 m (top) vs. modified roughness of 2 m (bottom) at 13 UTC term of forecast for 30 Mar 2005.

A relatively flat maximum during 09-12 UTC is observed for CPH, and at 12 UTC - for MAL. For roughness of 1 m, the average differences in velocities are 1.8 ± 0.4 m/s and 1.4 ± 0.5 m/s for CPH and MAL, respectively. For roughness of 2 m, the average changes in velocities are 2.4 ± 0.6 m/s and 2 ± 0.6 m/s for the same urban areas, respectively. Moreover, for both roughness values this difference is on average 1.3 times larger for CPH compared with MAL.

For temperature, a change in roughness does not contribute significantly compared with wind (Tab. 4.2.1). On a daily cycle, for both roughness values, approximately on average these differences are 0.14 ± 0.17ºC and 0.05 ± 0.09ºC for CPH and MAL, respectively. Although mostly the difference is positive, during 12-15 UTC the increased roughness slightly increasing temperature over the urbanized areas

Difference in fields	**Wind velocity at 10 m [m/s]**				**Temperature at 2 m [ºC]**			
Roughness, z_0	1 m		2 m		1 m		2 m	
Urban Area / **UTC term**	CPH	MAL	CPH	MAL	CPH	MAL	CPH	MAL
00	1.59	1.09	2.15	2.04	0.00	0.00	0.00	0.00
03	1.82	1.35	2.42	1.81	0.14	0.05	0.20	0.07
06	2.01	1.30	2.30	1.73	0.08	0.03	0.13	0.05
09	2.46	2.15	3.31	2.96	0.00	0.00	0.00	0.00
12	2.42	2.21	3.34	3.08	–0.05	–0.03	–0.07	–0.03
15	2.07	1.99	2.86	2.76	0.00	–0.02	0.00	–0.03
18	1.56	1.22	2.01	1.64	0.28	0.21	0.37	0.27
21	1.36	0.90	1.76	1.17	0.22	0.08	0.28	0.08
24	1.14	0.71	1.47	0.94	0.39	0.17	0.50	0.16

Tab. 4.3.1. Diurnal variation of difference fields for wind velocity at 10 m and temperature at 2 m for roughness values of 1 and 2 m for the CPH and MAL urbanized areas.

Albedo

Changes in albedo have the highest influence on the temperature field over the urbanized areas between 09-15 UTC, reaching during this time the maxima of difference in 2 and 1.8ºC for CPH and MAL, respectively. But it is less than 0.5ºC during the late evening – early morning period. Similarly, for wind velocities, except, that the difference between wind velocity fields is often more than two times larger for CPH vs. MAL urbanized areas. The maxima of difference are 1.6 and 0.8 m/s for CPH and MAL, respectively, and both are observed at 15 UTC. But this difference is less than 0.2 m/s during the late evening – early morning period.

Anthropogenic Heat Flux

As seen in Fig. 4.3.2, the incorporation (in the ISBA scheme) of anthropogenic flux for urban cells of modeling gridded domain shows well pronounced differences for simulated wind fields at 10 m. Note that, for this specific date, starting of 16 UTC term the difference became visible, at first, over the CPH urban area and it is approximately of 0.5 m/s. Then, the area extended faster more toward the inland of the Island of Zeeland and rapidly increases up to 1.5 m/s at 18 UTC. It is also became well pronounced over and to the west of MAL (up to 1.5 m/s). During the late evening – night – early morning hours the difference became the largest reaching a maximum of 2.1 m/s, and again by 10 UTC there is no difference visible between two runs. For anthropogenic fluxes of smaller magnitudes (i.e. for 100, 50, and 10 W/m^2) the highest difference (during the night time) reaches 1.6, 0.8, and 0.2 m/s. Moreover, this difference is slightly higher (by 0.1-0.2 m/s) for MAL compared with CPH.

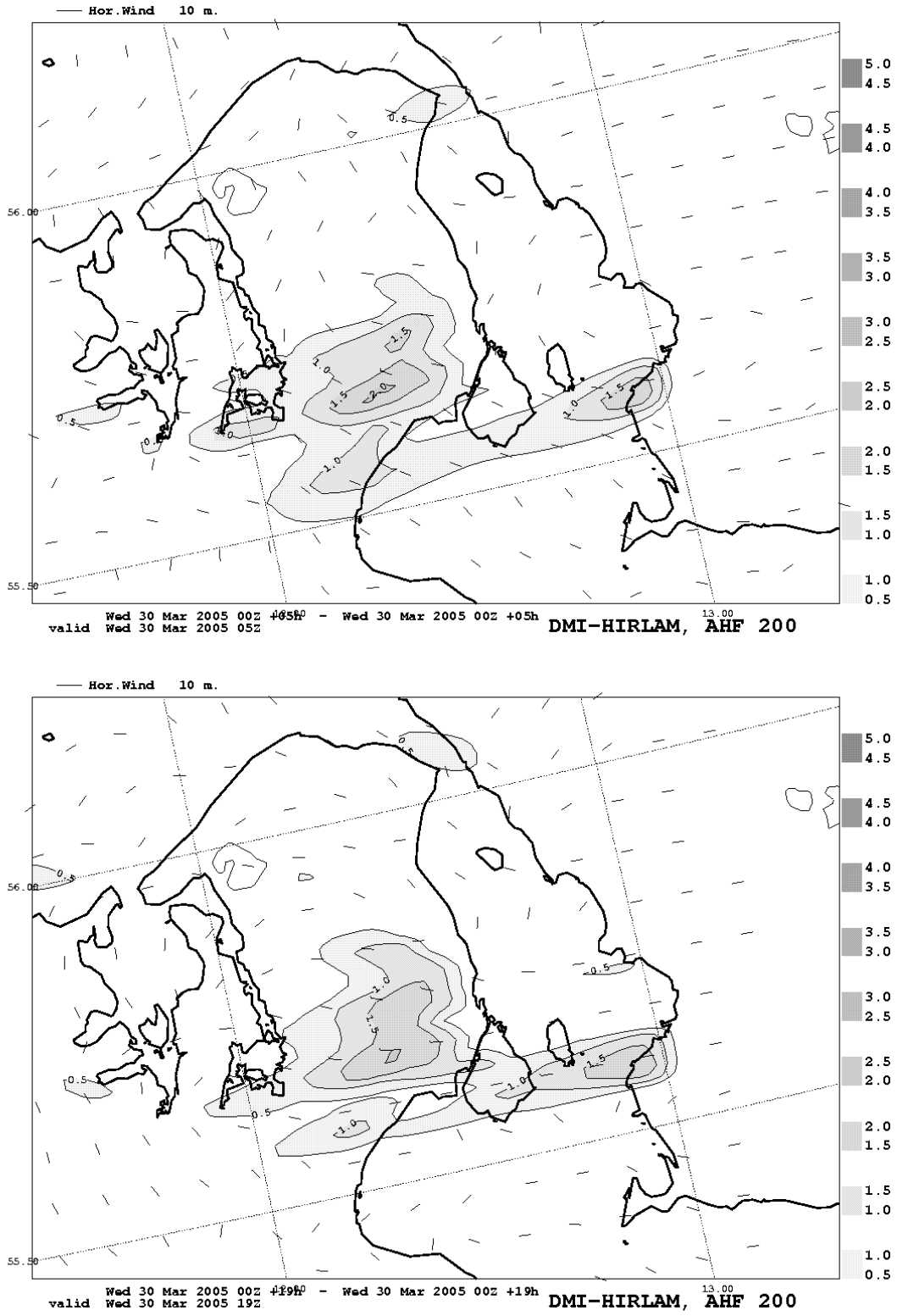

Fig. 4.3.2. Difference plots (between runs: DMI-HIRLAM control and added anthropogenic flux of 200 W/m^2) for wind velocity at 10 m at 05 UTC (top) and 19 UTC (bottom) forecasts for 30 March 2005.

For temperature (Tab. 4.3.2), for all terms the anthropogenic flux addition increases the temperature above the urban cells, except that it is smaller during 09-15 UTC with a minimum at noon. On average, it is higher for CPH compared with MAL. For a given range of selected anthropogenic fluxes, the diurnal average increase in temperature at 2 m varies from 0.09 ± 0.05 to 1.1 ± 0.6ºC for

the CPH urban area. For MAL, it is comparable with CPH – i.e. from 0.08 ± 0.05 to 1 ± 0.7ºC, although for higher values of anthropogenic flux the variability became larger. The range of maximum possible temperature increase varies within 0.15-1.93ºC and 0.15-2.27ºC for CPH and MAL, respectively. Moreover, on average, this increase is 1.1-1.4 times larger for CPH compared with MAL.

Anthropogenic heat flux [W/m^2]	200		100		50		10	
Urb Area UTC term	CPH	MAL	CPH	MAL	CPH	MAL	CPH	MAL
03	–1.36	–1.27	–0.87	–0.80	–0.50	–0.42	–0.11	–0.09
06	–1.36	–1.34	–0.90	–0.87	–0.53	–0.49	–0.11	–0.10
09	–0.70	–0.40	–0.38	–0.22	–0.20	–0.12	–0.04	–0.03
12	–0.38	–0.24	–0.20	–0.13	–0.10	–0.06	0.00	–0.01
15	–0.41	–0.28	–0.22	–0.15	–0.12	–0.08	–0.02	–0.02
18	–1.12	–0.78	–0.84	–0.54	–0.54	–0.37	–0.12	–0.09
21	–1.75	–1.66	–1.24	–1.20	–0.80	–0.71	–0.15	–0.15
24	–1.93	–2.27	–1.39	–1.59	–0.87	–0.77	–0.15	–0.13

Tab. 4.3.2. Diurnal variation of difference fields (in ºC) for temperature at 2 m for the anthropogenic flux values for the CPH and MAL urbanized areas.

As shown in Fig. 4.3.3 and Tab. 4.3.3, the anthropogenic flux contribution modifies also the latent heat flux over the grid cells of urbanized areas (it is well underlined by izolines around the CPH and MAL) and surroundings. The higher will be the magnitude of anthropogenic flux added, the longer time will be visible the influence on a diurnal cycle. This effect is more pronounced during the night time. For latent heat flux, the addition of anthropogenic flux modifies the latent heat flux in the urban cells, except that during the daytime its influence became randomly distributed over urbanized areas and almost disappears, especially during 12-15 UTCs. And it is increased at 09 UTC. On average, it is higher for CPH compared with MAL. For a given range of selected anthropogenic fluxes, the diurnal average decrease in latent heat flux is up to 22.2 and 17.9 W/m^2 for the CPH and MAL urban areas, respectively, with a large variance. In addition, the analysis of sensible heat flux showed, as expected, that over the urbanized areas (where the highest representation of urban class in the cell) this flux might be additionally changed up to 200 W/m^2.

Anthropogenic heat flux, W/m^2	200		100		50		10	
Urban Area UTC term	CPH	MAL	CPH	MAL	CPH	MAL	CPH	MAL
03	17.45	15.04	9.49	8.46	4.81	3.81	1.05	0.82
06	21.36	17.87	12.64	11.22	6.36	4.55	1.28	0.84
09	–15.50	–6.22	–14.82	–3.43	–8.92	–1.83	–1.99	–0.56
12	±5	±5	±1	±1	±1	±1	±0.2	±0.2
15	±5	±5	±1	±1	±1	±1	±0.2	±0.2
18	2.38	6.41	3.42	6.0	1.0	2.5	0.43	0.50
21	22.17	12.50	14.64	8.17	7.41	3.0	1.27	0.75
24	17.65	8.47	8.96	4.0	5.78	2.0	1.73	0.33

Tab. 4.3.3. Diurnal variation of difference fields (in W/m^2) for the latent heat flux at the surface for the anthropogenic flux values for the CPH and MAL urbanized areas.

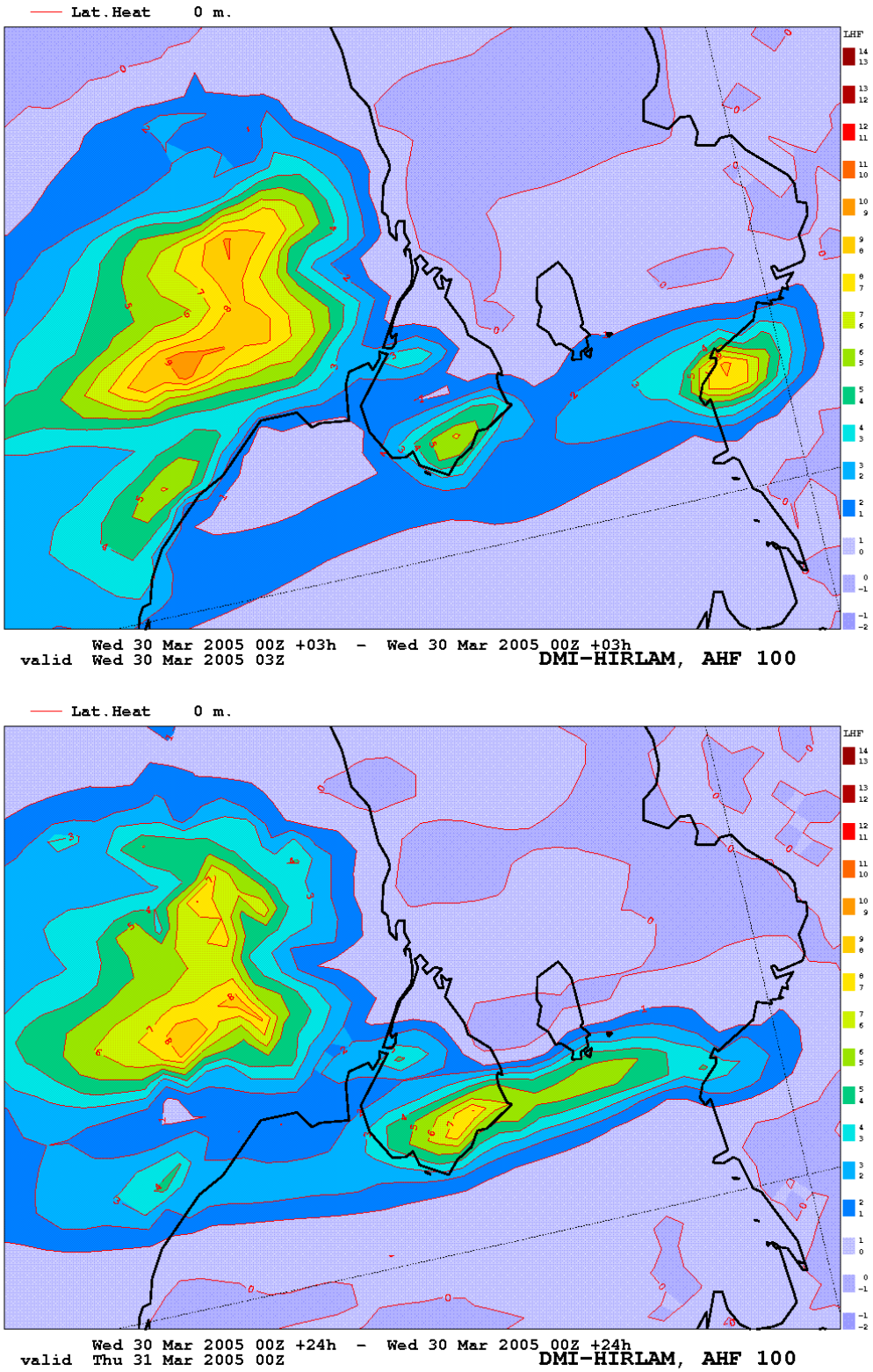

Fig. 4.3.3. Difference plots (between runs: DMI-HIRLAM control and added anthropogenic flux of 100 W/m^2) for latent heat flux at the surface for 03 UTC (top) and 24 UTC (bottom) forecasts for 30 March 2005.

4.4. Comparison of DMI-HIRLAM-S05 vs. U01 Long-Term Simulation of Diurnal Cycle in May-June 2005

The analysis of the DMI-HIRLAM-U01 simulation results vs. observational data and DMI-HIRLAM-S05 and D05 model outputs was performed considering a diurnal cycle of the temperature and relative humidity at 2 m, wind velocity at 10 m, and mean sea level pressure. These were evaluated as for the whole dataset of stations as well as for the coastal and land locations of stations (list of such Danish stations is shown, for example, in *Nielsen & Amstrup, 2004*) vs. observational data. In general, a more detailed information in other DMI-HIRLAM reports corresponding to different time periods and used models is given at http://origin1.dm.dk/~hirlam/ (internal DMI website). Let us consider these results as a preliminary evaluation, since in total only a relatively short time period during May-June 2005 is considered, assuming that further simulations employing the high resolution model will be continued during summer of 2005 as well as for July-August 2004, and statistics might be updated subsequently. Note, in June the upgraded DMI-HIRLAM-S05 model was run with the same setup (March-April-May of 2005) as the DMI-HIRLAM-U01 research version.

Temperature at 2 m

As shown in Fig. 4.4.1 (top-left), during May, the diurnal cycle of average temperature at 2 m is relatively well predicted by the S05 model compared with the others considered. For U01, the best fit with observational data is between 11 UTC and 19 UTC, and during the rest of the day it showed the underestimation of temperature (with temperature differences of more than 1ºC between 02 and 05 UTC). During June, the U01 model overestimated temperature during all diurnal cycle. Comparison of the coastal vs. land stations underlined the following (figures are available, but not shown). For the coastal stations, during May, all considered models underestimated temperature (with the highest for U01). In opposite, during June, the U01 model represented a relatively good fit to observational data, especially between 06-18 UTCs. For the land stations, during May, only D05 was characterized by the best fit to observational data compared with S05 and U01. Similar situation was observed in June, except that the U01 model always overestimated temperature (with a maximum of up to three degrees in the middle of the day). It should be noted that the diurnal variation of bias and rms for forecasts in May and June (figures are not shown) was better for S05 compared with U01, moreover, for temperature the performance of the U01 model in June was even worse (up to 2.7 and 1.5ºC for rms and bias, respectively).

Wind velocity at 10 m

As seen in Fig. 4.4.1 (bottom-left), during May, the diurnal cycle of average wind velocity at 10 m was well predicted by the U01 model compared with S05. Similar situation was observed during June, except that between 09-19 UTCs the S05 model showed better results with respect to observations. On a diurnal cycle of May, the maxima of wind velocity were observed in the middle of the day corresponding to 6.4 (6.4) vs. 6.1 m/s for the U01 (S05) models vs. observational data. The minima were observed at night corresponding to 3.5 (4.1) vs. 3.6 m/s for the U01 (S05) models vs. observational data. On a diurnal cycle of June, the maxima of wind velocity were also observed in the middle of the day corresponding to 6.1 (5.9) vs. 5.7 m/s for the U01 (S05) models vs. observational data. The minima were observed at night corresponding to 4.3 (4.8) vs. 4 m/s for the U01 (S05) models vs. observational data. It should be noted that the diurnal variation of bias and rms for forecasts in May and June (figures are not shown) was comparable, although for wind velocity the performance of the U01 model for both May and June was better (average rms of 0.2 and 0.4 m/s for May and June, respectively). On average, the bias for both models was around 1.5-1.6 m/s during May-June.

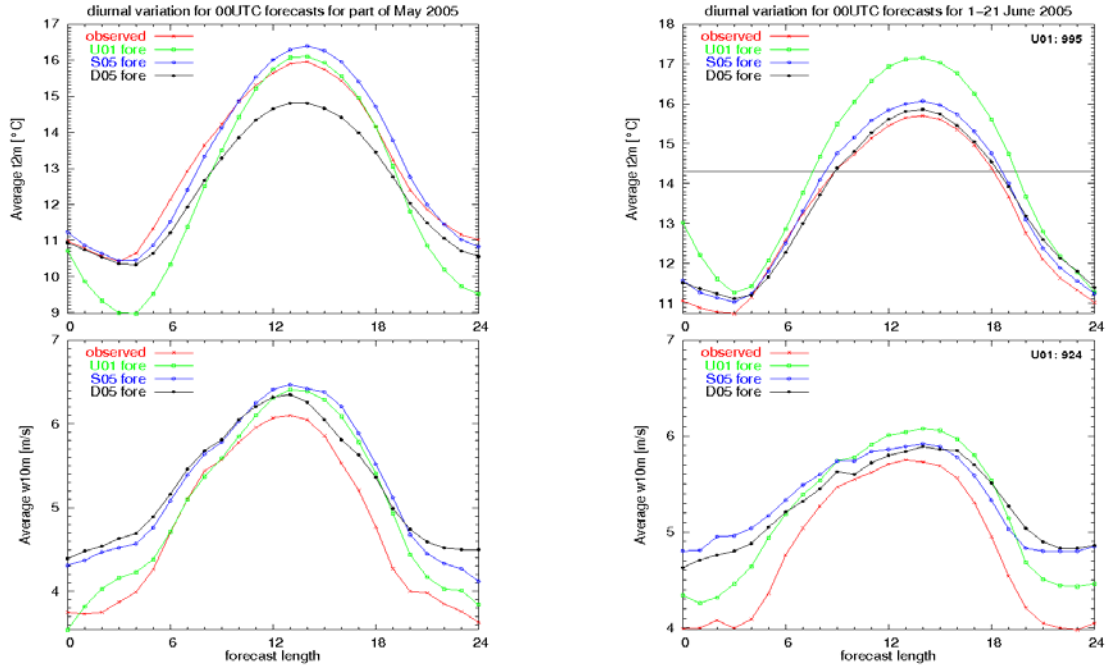

Fig. 4.4.1. Diurnal variation for 00 UTC forecasts of average temperature (in ºC) at 2 m (top) and average wind velocity (in m/s) at 10 m (bottom) based on the observational data and DMI-HILRAM-S05, -U01, and -D05 models for the studied periods of May 2005 (left) and June 2005 (right).

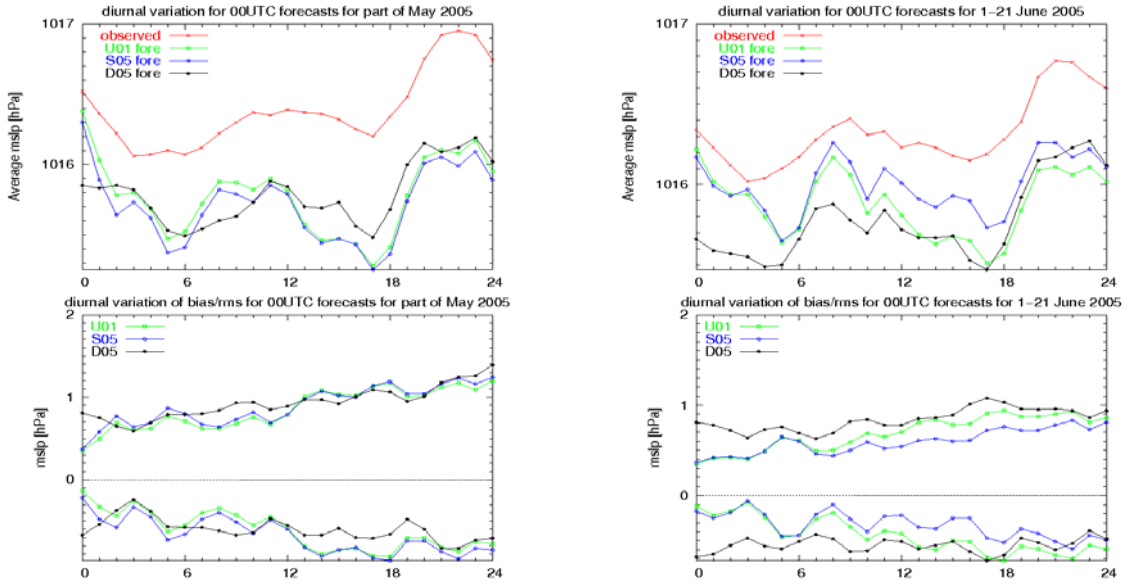

Fig. 4.4.2. Diurnal variation for 00 UTC forecasts of average mean sea level pressure (in hPa) (top) and bias/rms of pressure (in hPa) (bottom) based on the observational data and DMI-HILRAM-S05, -U01, and -D05 models for the studied periods of May 2005 (left) and June 2005 (right).

Mean Sea Level Pressure

As seen in Fig. 4.4.2 (top), during May, the diurnal cycle of mean sea level pressure was rela-

tively well predicted by both models compared with observational data (of less than 1 hPa), although U01 showed slightly better results. In June, it was better predicted by the S05 model compared with both U01 and D05. It should be noted that the diurnal variation of bias and rms for forecasts in May and June (Fig. 4.4.2 bottom) was comparable, although for pressure the performance of the models in May was slightly better, and moreover, in June after 06 UTC the S05 model showed lower bias and rms compared with other two models (which may be due to old vs. new setups for models runs).

Relative humidity at 2 m

As shown in Fig. 4.4.3 (top-left), during May, the diurnal cycle of average relative humidity at 2 m was not well predicted by both the S05 and U01 models (but comparable between these two models), especially between 09 and 20 UTC. The performance of the D05 model was better with respect to observational data. Since the U01 setup remained the same during June, the prediction of relative humidity by U01 was not improved as seen in Fig. 4.4.3 (top-right). In May, for the coastal stations, the S05 and U01 models performed better compared to the D05 model (Fig. 4.4.3 bottom-left), although this one is better in prediction for the land stations (Fig. 4.4.3 middle-left). Similarly, except the U01 model, is for June as shown in Fig. 4.4.3 (bottom/middle-right).

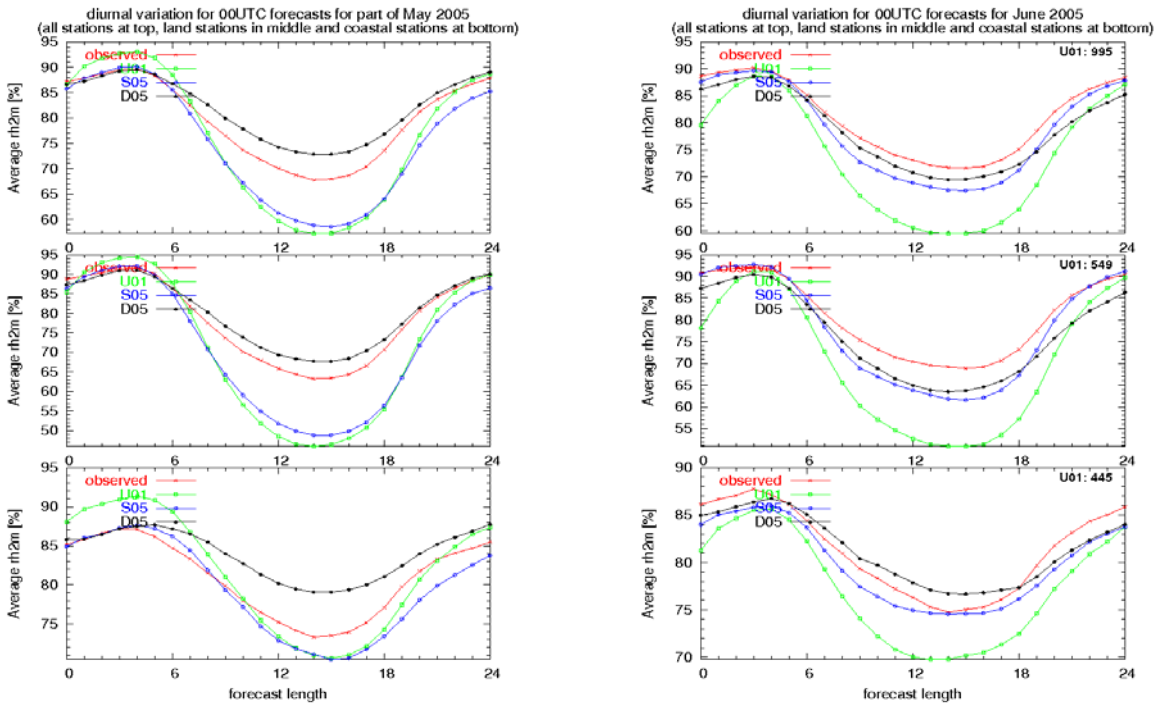

Fig. 4.4.3. Diurnal variation for 00 UTC forecasts of relative humidity (in %) at 2 m for the all (top), land (middle) and coastal (bottom) stations based on the observational data and DMI-HILRAM-S05, -U01, and -D05 models for the studied periods of May 2005 (left) and June 2005 (right).

Finally, we should briefly note and summarize for the U01 vs. S05 models, that:

- both simulated the average temperature and wind velocity are within an accuracy of forecast;
- mean sea level pressure simulated is in a good correspondence with observational data;
- both models do not differ in physics and parameterizations used as well as setups, except of more detailed climate generation files produced for the domain of higher resolution;
- U01 requires more of computational expenses compared with the S05 model.

Hence, it might be assumed that instead of the U01 model the S05 model can be used over the large scale domain of Denmark including Island of Bornholm. Although, for the extended urbanized areas (such as the Copenhagen, Århus, Odense, etc. metropolitan areas) the high resolution modelling might be considered for runs on smaller size domains employing similarly the boundary conditions of the S05 model and improved urban parameters descriptions in the DMI-HIRLAM ISBA land surface scheme.

Note, the high resolution simulations will be also useful to employ for the "concerned" areas (such as, for example, over the water and seashore surfaces of the Kattegat Passage and between Islands of Zeeland and Bornholm) where the high resolution simulations showed the highest deviations and discrepancies compared with the low resolution simulations. For this additional analysis of the time series of observational vs. simulated data will be needed.

Moreover, additional tests/verification of the DMI-HIRLAM-U01 high resolution model is needed, as performed now for the July-August 2004 period, and simulations continued through summer of 2005.

5. Concluding Remarks

In this technical report, several aspects of independent preparation of setups for new research modelling domains, land use classification and climate generation on examples of high resolution domains were presented. The DMI-HIRLAM model was run in research and short/long-term modes. Long-term simulations over the U01 domain were performed and then compared with outputs of the S05 model for several meteorological variables in the surface layer with observational data. Specific case study of typical and low wind conditions as well as May-June of 2005 time series were analysed on a diurnal cycle. Sensitivity tests of the ISBA land surface scheme of HIRLAM model were done also on examples of specific dates and for several parameters such as roughness, albedo, and anthropogenic heat fluxes. Research activities on this topics resulted in two submitted presentations and two manuscripts (mentioned in introduction section of Chapter 4 of this report).

6. Acknowledgments

The authors are grateful to Drs. Leif Laursen and Jens H. Sørensen of DMI, Patrice Mestayer, Sylvie Leroyer, and Nathalie Long (Ecole Centrale De Nantes, France) for collaboration, discussions and constructive comments. DMI research activities, shown in this technical report, are related to the high resolution modelling studies and are performed with the frameworks of the HIRLAM and FUMAPEX international projects.

The DMI-HIRLAM meteorological data were used as input data. The authors are grateful to the DMI Computer Support, HIRLAM group and Data Processing Department for the collaboration, computer assistance, and advice.

7. References

Amstrup B., **2004**: Validated meteorological input data provided by the larger scale models for the small scale models. *D10.5 FUMAPEX Deliverable* (DMI HIRLAM dataset). Danish Meteorological Institute, April 2004, Copenhagen, Denmark.

Baklanov A., A. Rasmussen, B. Fay, E. Berge, S. Finardi, **2002**: Potential and Shortcomings of Numerical Weather Prediction Models in Providing Meteorological Data for Urban Air Pollution Forecasting. *Water, Air and Soil Poll.: Focus*, 2(5-6): pp. 43-60.

Baklanov A., Mahura A., Petersen C., Sattler K., N.W. Nielsen, **2005**: Effects of Urbanized Areas

for NWP-DMI-HIRLAM High Resolution Model Operational Runs. *Manuscript in Preparation for Journal of Applied Meteorology*, 10 p.

Baklanov, A., P. Mestayer (editors), **2004**: Improved parameterisations of urban atmospheric sublayer and urban physiographic data classification. / A. Baklanov, E. Batchvarova, I. Calmet, A. Clappier, J.V. Chordá, J.J. Diéguez, S. Dupont, B. Fay, E. Fragkou, R. Hamdi, N. Kitwiroon, S. Leroyer, N. Long, A. Mahura, P. Mestayer, N.W. Nielsen, J.L. Palau, G. Pérez-Landa, T. Penelon, M. Rantamäki, G. Schayes, R.S. Sokhi. *D4.1, 4.2 and 4.5 FUMAPEX Report*, April 2004, Copenhagen, DMI, Denmark. *DMI Scientific Report* 04-05, ISBN - 87-7478-506-0.

Bringfelt B., **1996**: Tests of a New Land Surface Treatment in HIRLAM. *HIRLAM Technical Report*, 23, Norrköping, Sweden.

Dickinson R. E., A. Henderson-Sellers, P. J. Kennedy, M. F. Wilson, **1986:** Biosphere Atmosphere Transfer Scheme (BATS) for the NCAR Community Climate Model. *Technical Report of the National Center for Atmospheric Research*, NCAR, TN275.

Dickinson R. E., A. Henderson-Sellers, P. J. Kennedy, M. F. Wilson, **1993:** Biosphere-Atmosphere Transfer Scheme (BATS) version 1e as coupled to the NCAR Community Climate Model. *Technical Report of the National Center for Atmospheric Research*, NCAR TN387.

Fay B., L. Neunhäuserer, J. L. Palau, G. Pérez-Landa, J. J. Dieguez,V. Ødegaard,G. Bonafé, S. Jongen, A. Rasmussen, B. Amstrup, A. Baklanov, U. Damrath, **2005**: Evaluation and intercomparison of operational mesoscale models for FUMAPEX target cities. *FUMAPEX Report for D3.4,* DWD Offenbach, Germany, 110p.

Mahura A., Baklanov A., Petersen C., Sattler K., **2005a**: Effects of Urbanized Areas for High Resolution DMI-HIRLAM Simulations. *Abstracts of the European Meteorological Society 5th Annual Meeting, ECAM 7th EU Conference*, 12-16 September 2005, Utrecht, Netherlands, EMS05-A-00193.

Mahura A., Baklanov A., Petersen C., Sattler K., B. Amstrup, **2005b**: ISBA Scheme Performance in High Resolution Modelling for Low Winds Conditions. *HIRLAM Newsletters,* In Review, 6 p.

Mahura A., Baklanov A., S. Hoe, J.H. Sorensen, Petersen C., Sattler K., **2005c**: Evaluation of Land Surface Scheme Modifications on Atmospheric Transport and Deposition Patterns in Copenhagen Metropolitan Area. *Abstract submitted to 28th NATO/CCMS International Technical Meeting on Air Pollution Modelling and Its Applications*, 15-19 May 2006, Leipzig, Germany.

Mahura A., Mestayer, P.; Dupont, S.; Calmet, I.; Baklanov, A.; Leroyer, S.; Long, N.; Nielsen, N.W.; Sattler, K.; Petersen, C., **2005d**: Comparison of short and long-term modelled latent, sensible, and storage heat fluxes employing numerical weather prediction model with and without urbanized modules. *Manuscript in preparation for Atmospheric Chemistry and Physics.*

Mahura A., S. Leroyer, I. Calmet, P. Mestayer, A. Baklanov, C. Petersen, K. Satter, **2005e**: Large eddy simulation of typical climatological heat fluxes for urbanized areas. *Abstracts of the European Meteorological Society 5th Annual Meeting, ECAM 7th EU Conference*, 12-16 September 2005, Utrecht, Netherlands, EMS05-A-00253.

Mahura A., Leroyer S., Mestayer P., Calmet I., Dupont S., Long N., Baklanov A., Petersen C., Sattler K., Nielsen N.W. **2005f**: Large Eddy Simulation of Urban Features for Copenhagen Metropolitan Area. *Atmospheric Chemistry and Physics Discussions, Vol 5, pp 1-31, In Peer-review.*

METGRAF, DMI www site: http://origin1.dmi.dk/~hirlam/metgraf.html

Mogensen K., **2004**: Running and Installing Metgraf Ver2., *Internal DMI FM Memo*, 4 p. Contact: ksa@dmi.dk

Navascués B., Rodríguez E., J.J. Ayuso, S. Järvenoja, **2003**: Analysis of surface variables and parameterization of surface processes in HIRLAM. Part II: Seasonal assimilation experiment. Norrköping. *HIRLAM Technical Report* 59, 38 p.

NCSA, **1999a**: HDF Reference Manual, Version 4.1r3. *National Center for Supercomputing Applications, NCSA*. www : http://hdf.ncsa.uiuc.edu & http://hdf.ncsa.uiuc.edu/RefMan41r3_html/

NCSA, **1999b**: HDF User's Guide, Version 4.1r3. *National Center for Supercomputing Applications, NCSA*. www : http://hdf.ncsa.uiuc.edu & http://hdf.ncsa.uiuc.edu/UG41r3_html/

Nielsen N.W., B. Amstrup, **2004**: DMI-HIRLAM Verification/ Benchmarking Report for the first

Quarter of 2004. *DMI Intern Report* 04-11, 51 p.

Noilhan J., Mahfouf J.F., **1996**: The ISBA land-surface parameterization scheme. *Global and Planetary Change*, 13, 145-149.

Noilhan J., Planton S., **1989**: A simple parameterization of land surface processes for meteorological models. *Monthly Weather Review*, 117, pp. 536-549.

Rodríguez E., B. Navascués, J.J. Ayuso, S. Järvenoja, **2003**: Analysis of surface variables and parameterization of surface processes in HIRLAM. Part I: Approach and verification by parallel runs. Norrköping. *HIRLAM Technical Report* 58, 52 p.

Sass B., N.W. Nielsen, J.U. Jørgensen, B. Amstrup, M. Kmit, K.S. Mogensen, **2002**: The Operational DMI-HIRLAM System 2002-version. *Danish Meteorological Institute Technical Report*, 02-05, 60 p.

Sattler K., **1999**: New high resolution physiograpic data and climate generation for the HIRLAM forecast system. *Danish Meteorological Institute Technical Report*, 11-99, 43 p.

Sattler K.: **2000,** New high resolution physiographic data and climate generation in the HIRLAM forecasting system at DMI, an overview, *HIRLAM Newsletter*, 33, 96-100.

Undén P., L. Rontu, H. Järvinen, P. Lynch, J. Calvo, G. Cats, J. Cuhart, K. Eerola, etc. **2002**: HIRLAM-5 Scientific Documentation. December 2002, *HIRLAM-5 Project Report,* SMHI.

USGS, **1997**: The Global Land Cover Characteristics Database. *US Geological Survey, USGS.* www*:* http://edcdaac.usgs.gov/glcc/glcc.asp

USGS, **1998**: GTOPO30, Global 30 Arc Second Elevation Dataset. *US Geological Survey, USGS*. www*:* http://edcdaac.usgs.gov/gtopo30/gtopo30.asp

WMO, **1994**: GRIB - A Guide to the Code Form FM 92-IX Ext. GRIB, 1st Edition. *World Meteorological Organization, WMO*. www: http://www.wmo.ch/web/www/WMOCodes/Guides/GRIB/GRIB1-Contents.html

8. Appendixes

Appendix 1. Example of Calculation of Parameters for New Modelling Domain

Following formulations given in Chapter 2 of this report:

- Select resolution of new modelling domain (NMD) as ΔLON = ΔLAT (in degrees) = 0.014º
- Calculate total number of passive boundary points for NMD:
  if select NPBP = 4 (number of passive boundary points)
  NBNDRY = 2 · (NPBP + 1) = 2 · (4 + 1) = **10**
- Since selected number of grid points along longitude for DMI-HIRLAM NWP - $NLON_{NWP}$ - should satisfy a set of (n, m, p) conditions ($2^n \cdot 3^m \cdot 5^p$), check that - $NLON_{NWP}$ = 360 - this value exist/given in Table of Appendix 2 and for this value conditions are true:
  $2^n \cdot 3^m \cdot 5^p = 2^3 \cdot 3^2 \cdot 5^1 = 8 \cdot 9 \cdot 5 =$ **360**
- Calculate total number of grid points in NMD along longitude:
  $NLON_{NMD} = NLON_{NWP} + NBNDRY = 360 + 10 =$ **370**
- Calculate number of grid points /minus one/ in NMD along longitude:
  $NLON_{NMD}$ -1 = 370 – 1 **= 369**
  (*note: NLON must be even number*)
- Select the values for the south-east corner of NMD in rotated system of coordinates:
  EAST = 3.343 and SOUTH = 4.379
  (*note: values must be given in millidegrees*)
- By try/error/iteration select values for the WEST-EAST boundaries of NMD in the rotated system of coordinates that it should cover geographical area of interest and also satisfy condition:
  | WEST –EAST | / ΔLON = | –1.823 – 3.343 | / 0.014 = 5.166 / 0.014 **= 369**
  (*note: values must be given in millidegrees*)
- Calculate number of grid points /minus one/ in NMD along latitude:
  $NLAT_{NMD}$ –1 = 260 – 1 **= 259**
  (*note: NLAT must be even number*)
- By try/error/iteration select values for NORTH-SOUTH boundaries of NMD in the rotated system of coordinates that it should cover geographical area of interest and also satisfy condition:
  | NORTH – SOUTH | / ΔLAT = | 8.005 – 4.379 | / 0.014 = 3.626 / 0.014 **= 259**
  (*note: values must be given in millidegrees*)

Appendix 2. DMI-HIRLAM Model Conditions for Number of Grid Points along Longitude

#	$NLON_{NWP}$	p	m	n	#	$NLON_{NWP}$	p	m	n
1	20	1	0	2	*51*	750	3	1	1
2	24	0	1	3	*52*	768	0	1	8
3	30	1	1	1	*53*	800	2	0	5
4	32	0	0	5	*54*	810	1	4	1
5	36	0	2	2	*55*	864	0	3	5
6	40	1	0	3	*56*	900	2	2	2
7	48	0	1	4	*57*	960	1	1	6
8	50	2	0	1	*58*	972	0	5	2
9	54	0	3	1	*59*	1000	3	0	3
10	60	1	1	2	*60*	1024	0	0	10
11	64	0	0	6	*61*	1080	1	3	3
12	72	0	2	3	*62*	1152	0	2	7
13	80	1	0	4	*63*	1200	2	1	4
14	90	1	2	1	*64*	1250	4	0	1
15	96	0	1	5	*65*	1280	1	0	8
16	100	2	0	2	*66*	1296	0	4	4
17	108	0	3	2	*67*	1350	2	3	1
18	120	1	1	3	*68*	1440	1	2	5
19	128	0	0	7	*69*	1458	0	6	1
20	144	0	2	4	*70*	1500	3	1	2
21	150	2	1	1	*71*	1536	0	1	9
22	160	1	0	5	*72*	1600	2	0	6
23	162	0	4	1	*73*	1620	1	4	2
24	180	1	2	2	*74*	1728	0	3	6
25	192	0	1	6	*75*	1800	2	2	3
26	200	2	0	3	*76*	1920	1	1	7
27	216	0	3	3	*77*	1944	0	5	3
28	240	1	1	4	*78*	2000	3	0	4
29	250	3	0	1	*79*	2048	0	0	11
30	256	0	0	8	*80*	2160	1	3	4
31	270	1	3	1	*81*	2250	3	2	1
32	288	0	2	5	*82*	2304	0	2	8
33	300	2	1	2	*83*	2400	2	1	5
34	320	1	0	6	*84*	2430	1	5	1
35	324	0	4	2	*85*	2500	4	0	2
36	**360**	**1**	**2**	**3**	*86*	2560	1	0	9
37	384	0	1	7	*87*	2592	0	4	5
38	400	2	0	4	*88*	2700	2	3	2
39	432	0	3	4	*89*	2880	1	2	6
40	450	2	2	1	*90*	2916	0	6	2
41	480	1	1	5	*91*	3000	3	1	3
42	486	0	5	1	*92*	3072	0	1	10
43	500	3	0	2	*93*	3200	2	0	7
44	512	0	0	9	*94*	3240	1	4	3
45	540	1	3	2	*95*	3456	0	3	7
46	576	0	2	6	*96*	3600	2	2	4
47	600	2	1	3	*97*	3750	4	1	1
48	640	1	0	7	*98*	3840	1	1	8
49	648	0	4	3	*99*	3888	0	5	4
50	720	1	2	4	*100*	4000	3	0	5

Appendix 3. CORINE Land Cover Legend for I01 Modelling Domain

#		
#	**CORINE land cover legend**	**- Modified for I01 Modelling Domain**
#		
1	106	CONTINIOUS URBAN FABRIC
2	106	DISCONTINUOUS URBAN FABRIC
3	106	INDUSTRIAL OR COMMERCIAL ZONES
4	104	ROAD AND RAILNETWORKS AND ASSOCIATED LAND
5	104	PORT AREAS
6	104	AIRPORTS
7	105	MINERAL EXTRACTION SITES
8	105	DUMP SITES
9	105	CONSTRUCTION SITES
10	102	GREEN URBAN AREAS
11	102	SPORT AND LEISURE FACILITIES
12	105	NON-IRRIGATED ARABLE LAND
13	105	PERMANENTLY IRRIGATED LAND
14	103	RICE FIELDS
15	101	VINE YARDS
16	101	FRUIT TREES AND BERRY PLANTATIONS
17	103	OLIVE GROVES
18	103	PASTURES
19	103	ANNUAL CROPS ASSOCIATED WITH PERMANENT CROPS
20	103	COMPLEX CULTIVATION PATTERNS
21	103	LAND PRINCIPALLY OCCUPIED BY AGRICULTURE, WITH SIGN. AREAS OF NAT. VEGET.
22	103	AGRO-FORESTRY AREAS
23	101	BROAD-LEAVED FOREST
24	101	CONIFEROUS FOREST
25	101	MIXED FOREST
26	103	NATURAL GRASSLAND
27	103	MOORS AND HEATHLAND
28	101	SCLEROPHYLLOUS VEGETATION
29	101	TRANSITIONAL WOODLAND-SHRUB
30	105	BEACHES, DUNES, AND SAND PLAINS
31	105	BARE ROCK
32	103	SPARSELY VEGETATED AREAS
33	105	BURNT AREAS
34	105	GLACIERS AND PERPETUAL SNOW
35	103	INLAND MARSHES
36	105	PEATBOGS
37	105	SALT-MARSHES
38	105	SALINES
39	105	INTERTIDAL FLATS
40	107	WATER COURSES
41	107	WATER BODIES
42	107	COASTAL LAGOONS
43	107	ESTUARIES
44	107	SEA AND OCEAN
45	-	ignore
46	-	ignore
47	-	ignore
48	-	ignore
49	-	ignore
50	107	UNCLASSIFIED WATER BODIES
51	-	ignore
52	-	ignore
53	-	ignore
54	-	ignore

55 - ignore
56 - ignore
57 - ignore
58 - ignore
59 - ignore
60 - ignore
61 106 URBAN FABRIC
62 106 INDUSTRIAL, COMMERCIAL AND TRANSPORT UNITS
63 105 MINE. DUMP AND CONSTRUCTION SITES
64 104 ARTIFICIAL NON-AGRICULTURAL VEGETATED AREAS
65 105 ARABLE LAND
66 103 PERMANENT CROPS
67 103 PASTURES
68 103 HETEROGENEOUS AGRICULTURAL AREAS
69 101 FORESTS
70 103 SHRUB AND/OR HERBACEOUS VEGETATION ASSOCIATIONS
71 103 OPEN SPACES WITH LITTLE OR NO VEGETATION
72 103 INLAND WETLANDS
73 105 COASTAL WETLANDS
74 107 INLAND WATERS
75 107 MARINE WATERS
76 - ignore
77 - ignore
78 - ignore
79 - ignore
80 - ignore
81 104 ARTIFICIAL SURFACES
82 103 AGRICULTURAL AREAS
83 101 FORESTS AND SEMI-NATURAL AREAS
84 103 WETLANDS
85 107 WATER BODIES
86 - ignore
87 - ignore
88 - ignore
89 - ignore
90 - ignore
91 - ignore
92 - ignore
93 - ignore
94 - ignore
95 - ignore
96 - ignore
97 - ignore
98 - ignore
99 - ignore
100 - ignore
#
Climate generation classification (BATS-like) - for I01 Modelling Domain
#
101 v **vegn__veg_on_nat_soil**
102 v **vega__veg_on_art_soil**
103 v **nat__nat_soil_veg**
104 v **art__art_soil_veg**
105 b **bare__bare_soil**
106 u **bat__buildings**
107 w **eau__water**

Appendix 4. Reference to Records in Climate Generation File of GRIB-Format

Parameter	LevelType	Level	Description
6	105	0	surface geopotential
11	105	998	soil temperature second soil layer
86	105	998	soil water second soil layer
83	105	0	surface roughness
83	105	702	sea-surface roughness
84	105	0	surface albedo
196	105	0	fraction of lakes
81	105	901	fraction of water
199	105	901	vegetation type in tile (=14, new: 14,15)
195	105	901	soil type in tile (=99)
86	105	901	soil water content surface layer (=0.0)
86	105	951	soil water content second/third soil layer (=0.0)
193	105	901	frozen water in surface layer of tile
193	105	951	frozen water in total layer of tile
11	105	901	sea surface temperature
191	105	901	BATS1 primary land cover class or snow density? (=99)
190	105	901	snow albedo (=99)
11	105	951	sea temperature (=SST?)
66	105	901	snow depth in tile (=0.)
192	105	901	BATS2 secondary land cover class (=99)
81	105	902	fraction of ice
199	105	902	vegetation type in tile (=19)
195	105	902	soil type in tile (=99)
86	105	902	soil water content surface layer
86	105	952	soil water content second/third soil layer
193	105	902	frozen water in surface layer of tile
193	105	952	frozen water in total layer of tile
11	105	902	ice surface temperature
191	105	902	BATS1 primary land cover class or snow density? (=0.1)
190	105	902	snow albedo (=0.85)
11	105	952	ice temperature (=ice surface temperature?)
66	105	902	snow depth in tile
192	105	902	BATS2 secondary land cover class (=99)
81	105	903	fraction of bare soil
199	105	903	vegetation type in tile (8,12)
195	105	903	soil type in tile
86	105	903	soil water content surface layer
86	105	953	soil water content second/third soil layer
193	105	903	frozen water in surface layer of tile
193	105	953	frozen water in total layer of tile
11	105	903	soil surface temperature of tile
191	105	903	BATS1 primary land cover class or snow density? (=0.1)
190	105	903	snow albedo (=0.85)
11	105	953	soil temperature second soil layer in tile
66	105	903	snow depth in tile
192	105	903	BATS2 secondary land cover class (=99)
81	**105**	**904**	**fraction of low vegetation**
199	105	904	vegetation type in tile (1,2,7,9,10,11,13,16,17)
195	105	904	soil type in tile
86	105	904	soil water content surface layer
86	105	954	soil water content second/third soil layer
193	105	904	frozen water in surface layer of tile
193	105	954	frozen water in total layer of tile
11	105	904	soil surface temperature of tile
191	105	904	BATS1 primary land cover class or snow density? (=0.1)
190	105	904	snow albedo (=0.85)
11	105	954	soil temperature second soil layer in tile
66	105	904	snow depth in tile
192	105	904	BATS2 secondary land cover class (=0)
81	105	905	fraction of forest
199	105	905	vegetation type in tile (3,4,5,6,18)
195	105	905	soil type in tile
86	105	905	soil water content surface layer
86	105	955	soil water content second/third soil layer
193	105	905	frozen water in surface layer of tile
193	105	955	frozen water in total layer of tile
11	105	905	soil surface temperature of tile
191	105	905	BATS1 primary land cover class or snow density? (=0.1)
190	105	905	snow albedo (=0.85)
11	105	955	soil temperature second soil layer in tile
66	105	905	snow depth in tile
192	105	905	BATS2 secondary land cover class (=0)

Appendix 5. Wind and Temperature Fields for Typical Case Study

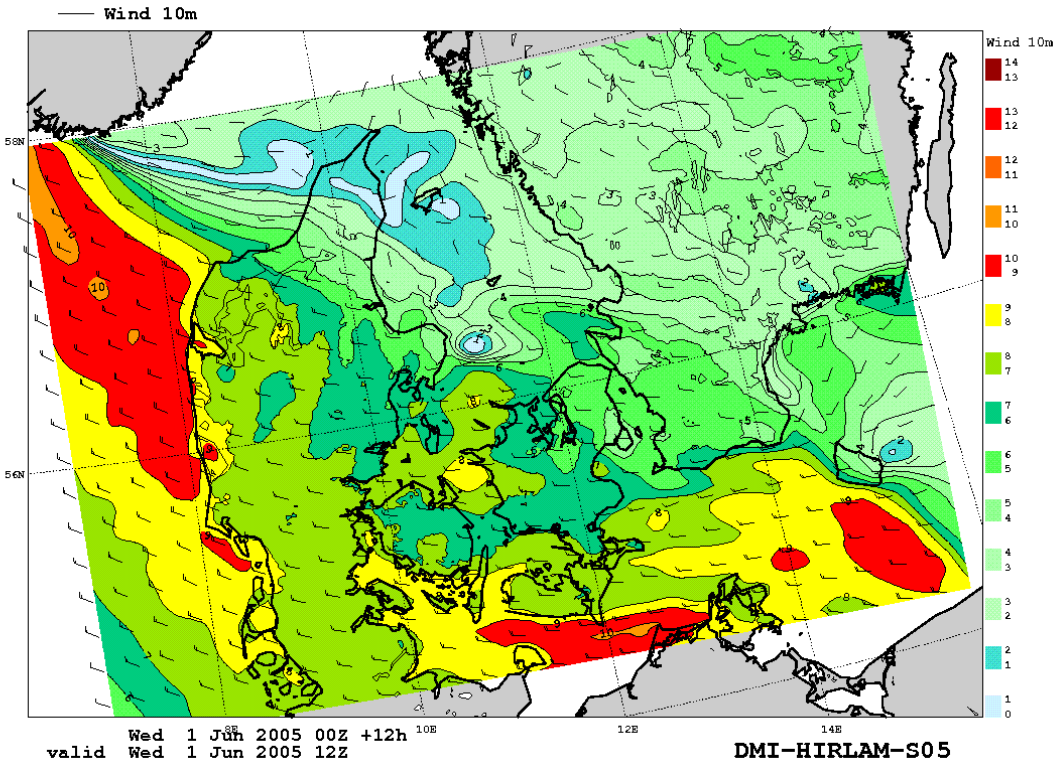

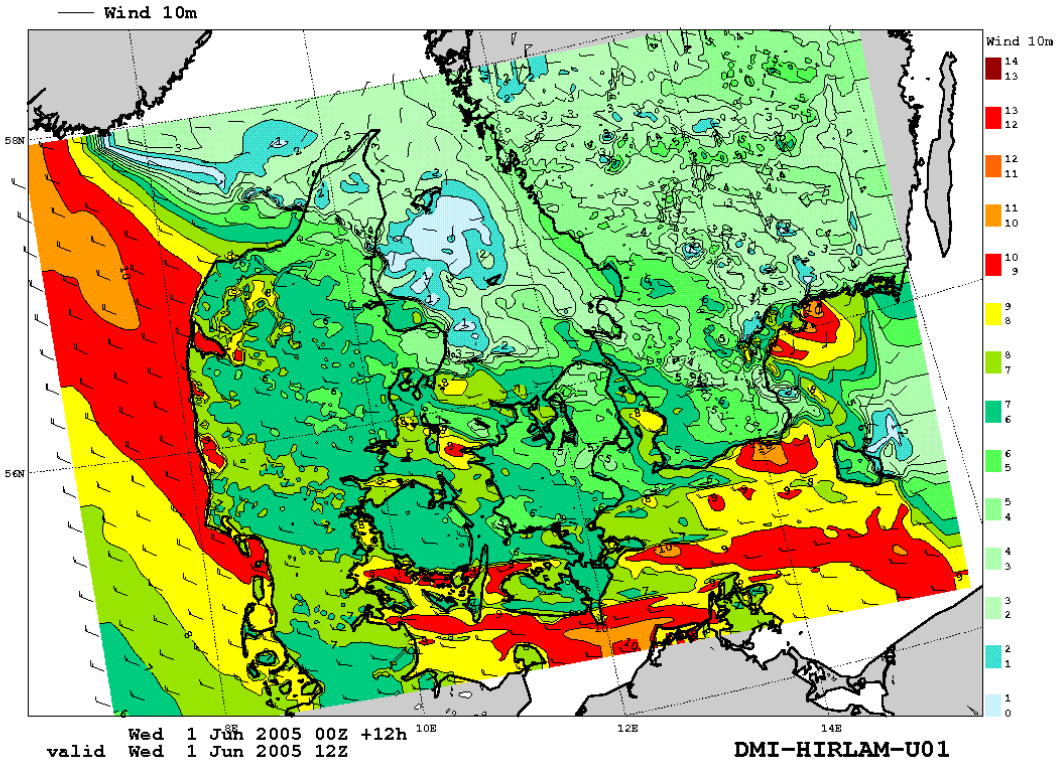

A5.1. Wind fields at 10 m over the U01 modelling domain simulated by the DMI-HIRLAM-S05 (top) and U01 (bottom) models at term of 12 UTC, 1 June 2005.

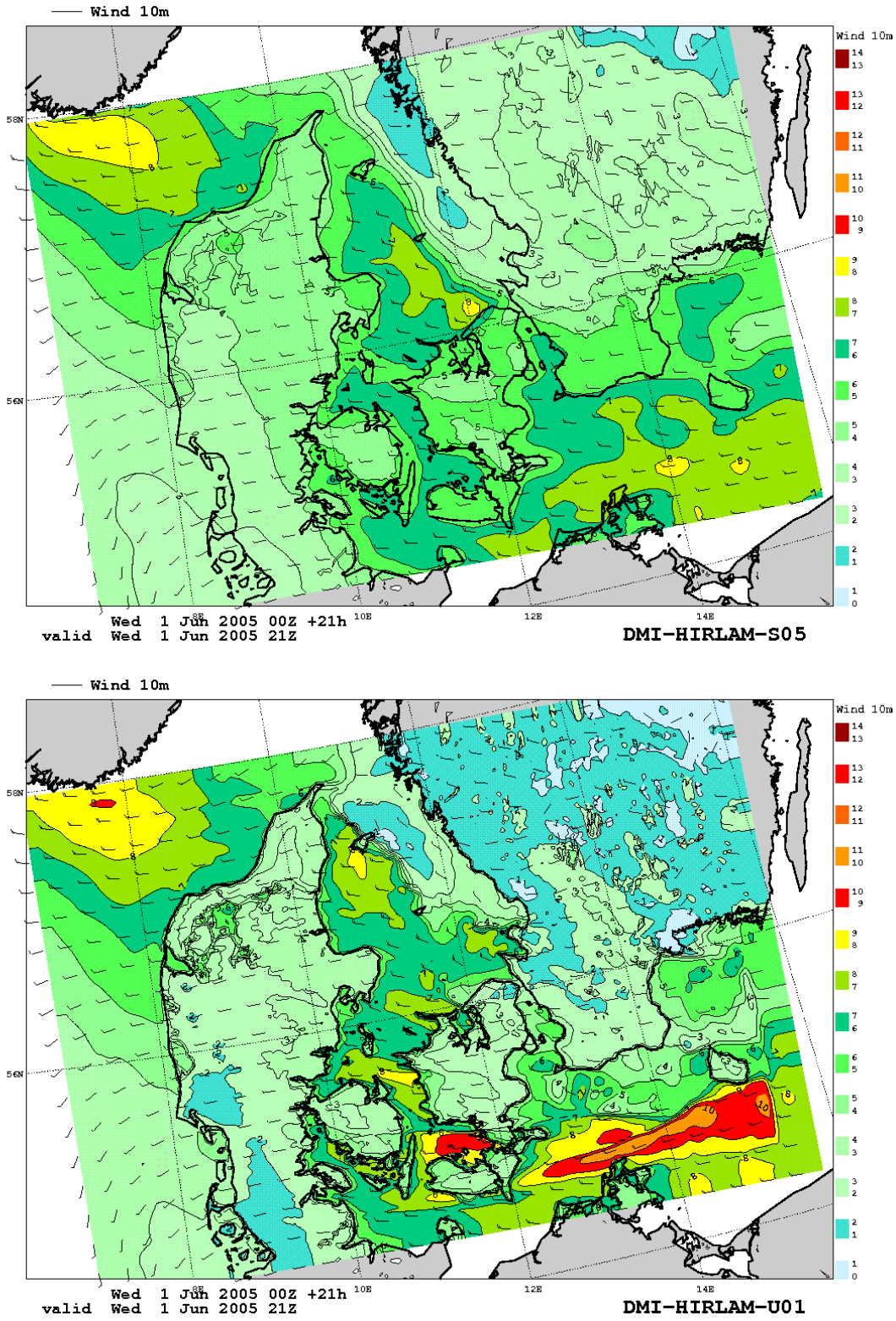

A5.2. Wind fields at 10 m over the U01 modelling domain simulated by the DMI-HIRLAM-S05 (top) and U01 (bottom) models at term of 21 UTC, 1 June 2005.

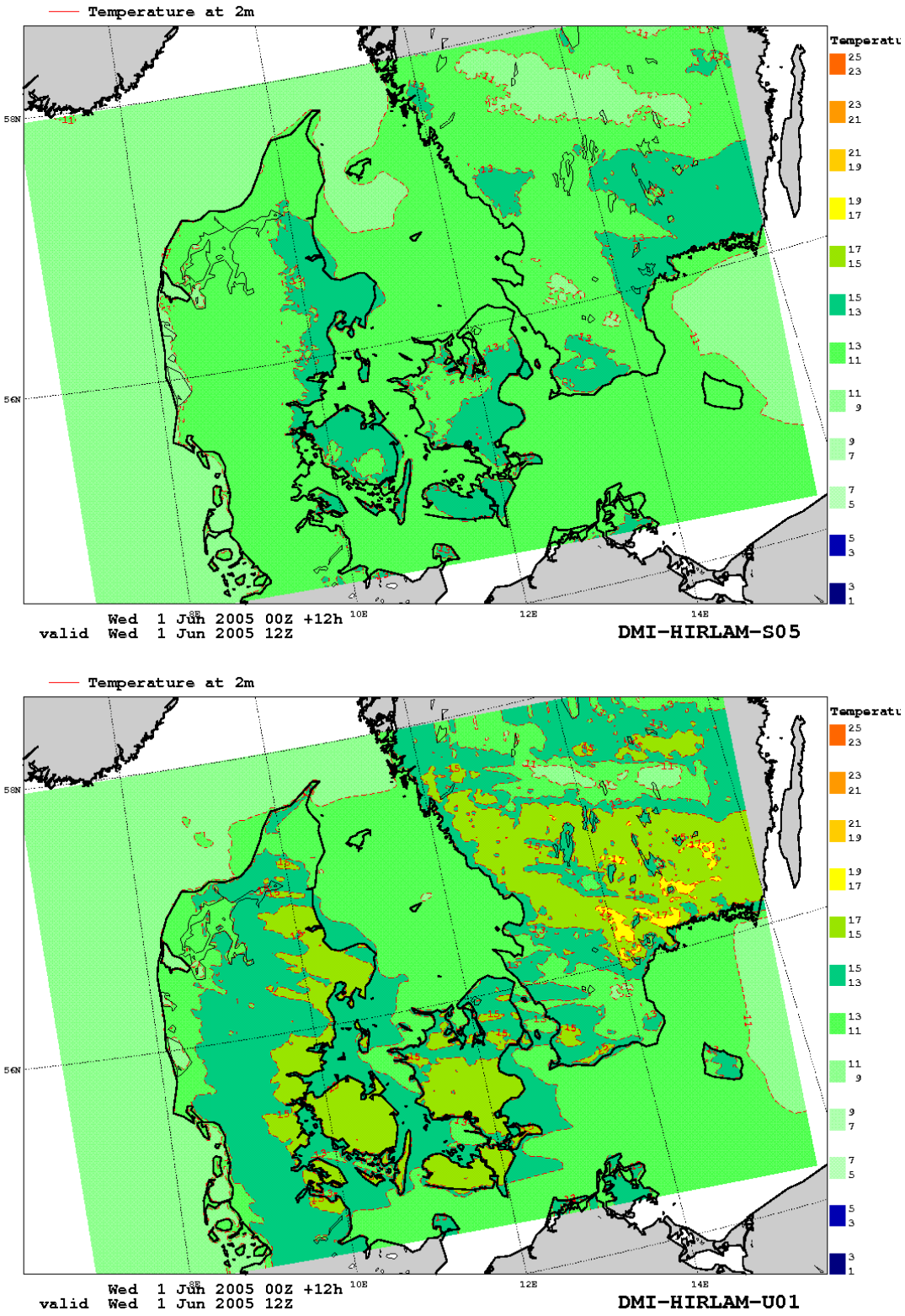

A5.3. Temperature fields at 2 m over the U01 modelling domain simulated by the DMI-HIRLAM-S05 (top) and U01 (bottom) models at term of 12 UTC, 1 June 2005.

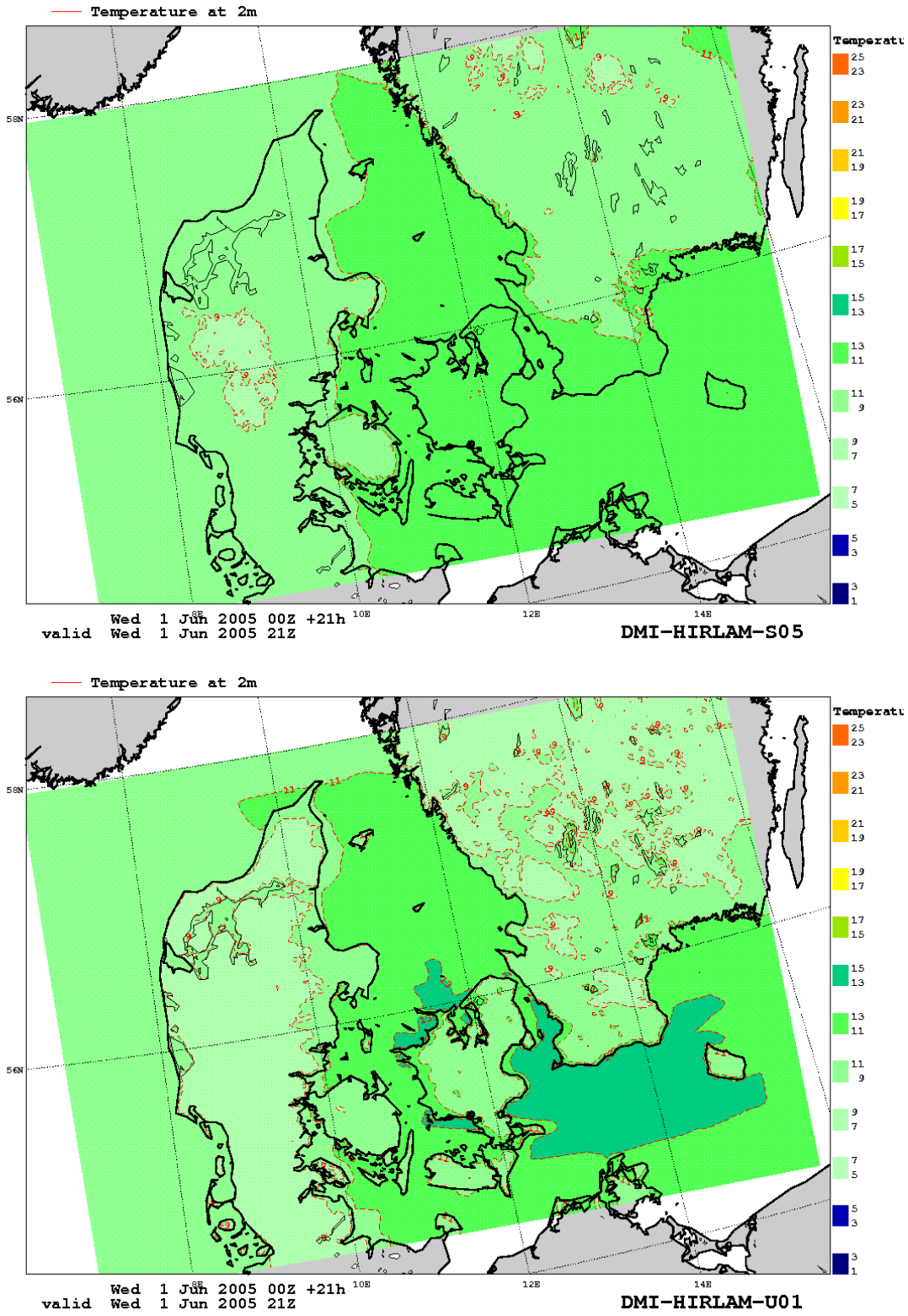

Fig. A5.4. Temperature fields at 2 m over the U01 modelling domain simulated by the DMI-HIRLAM-S05 (top) and U01 (bottom) models at term of 21 UTC, 1 June 2005.

Appendix 6. Wind and Temperature Fields for Specific Case Study of Low Wind Conditions

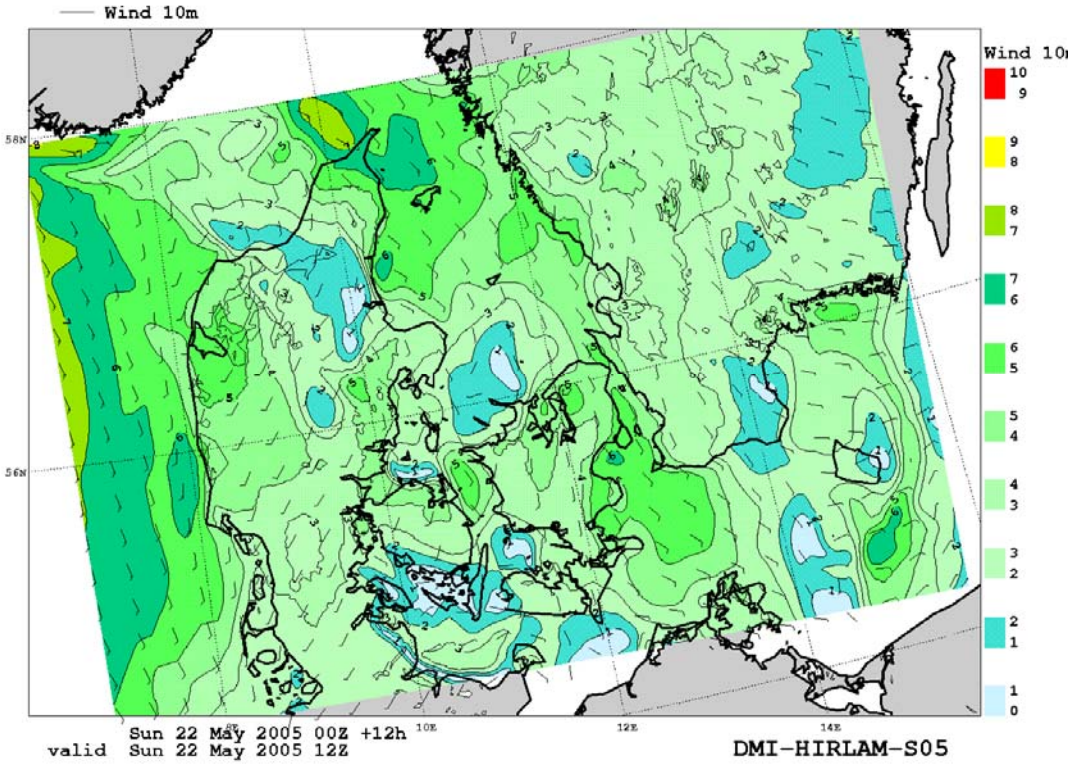

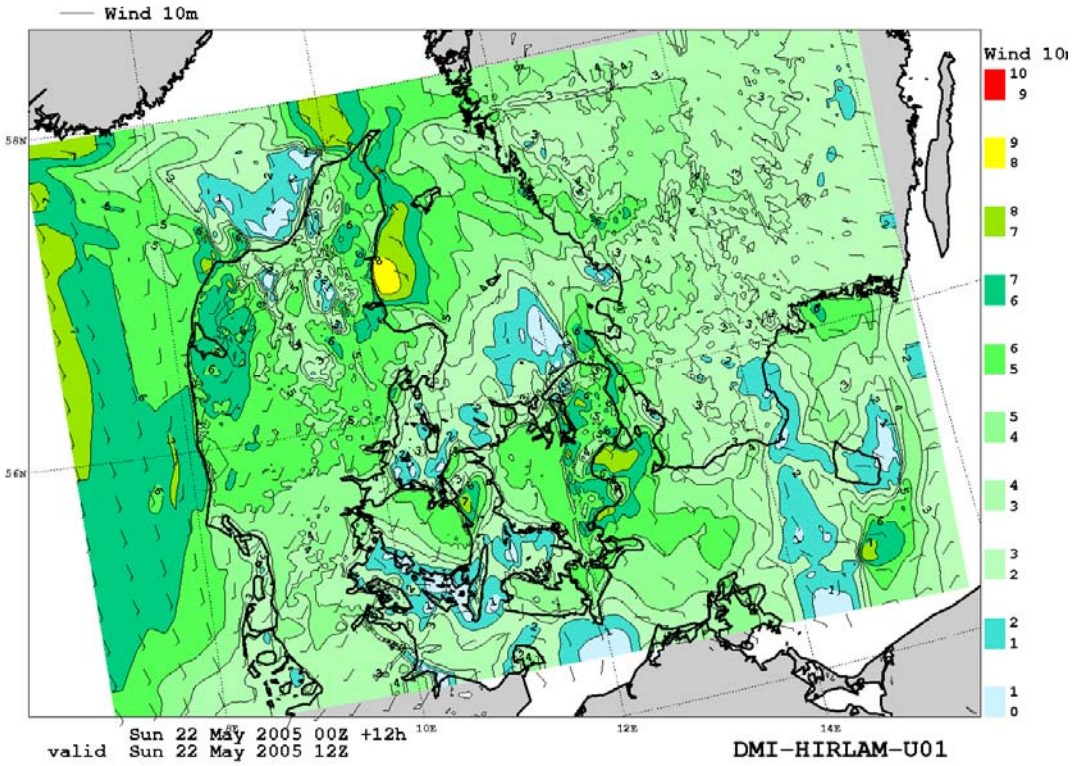

A6.1. Wind fields at 10 m over the U01 modelling domain simulated by the DMI-HIRLAM-S05 (top) and U01 (bottom) models at term of 12 UTC, 22 May 2005.

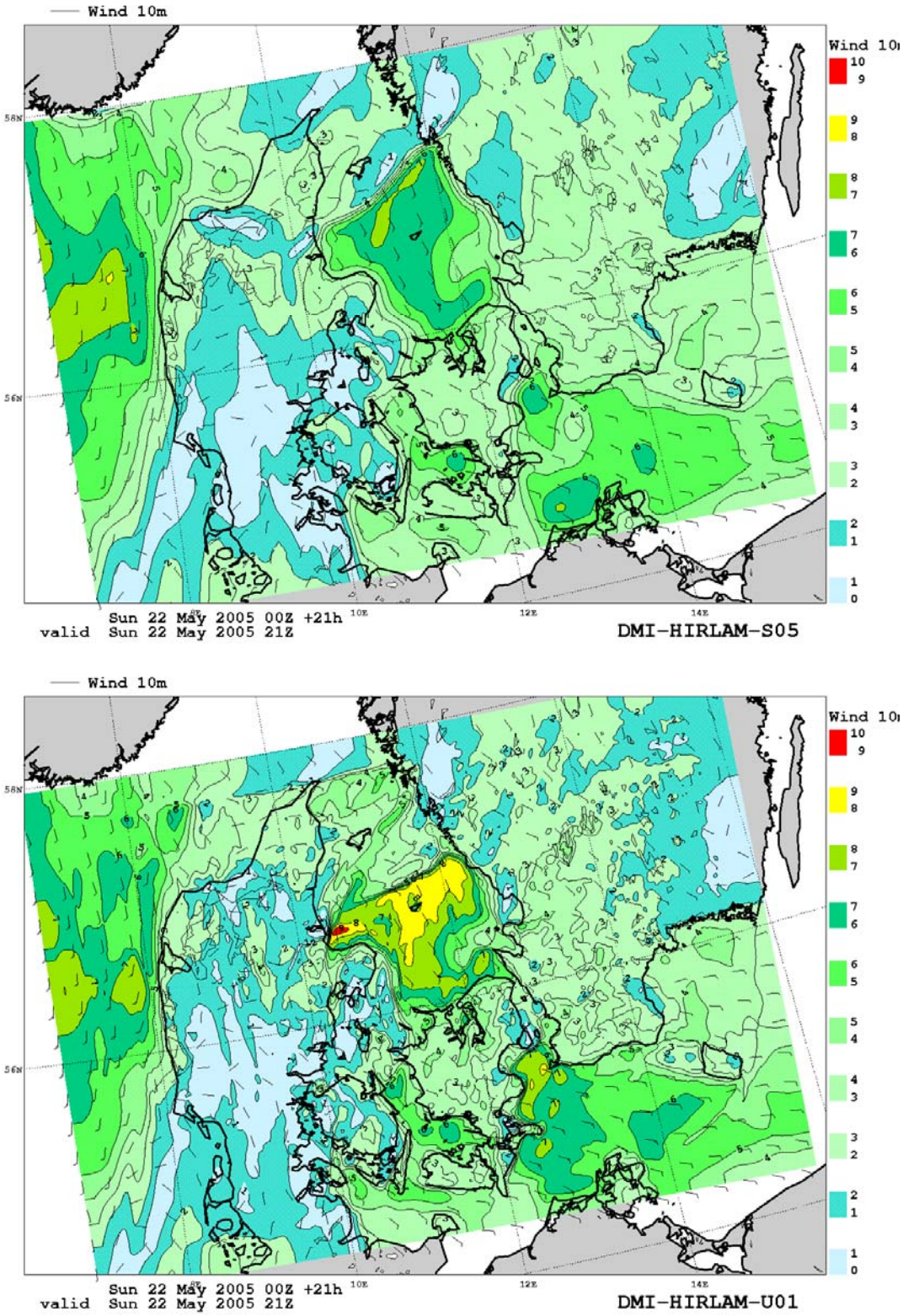

A6.2. Wind fields at 10 m over the U01 modelling domain simulated by the DMI-HIRLAM-S05 (top) and U01 (bottom) models at term of 21 UTC, 22 May 2005.

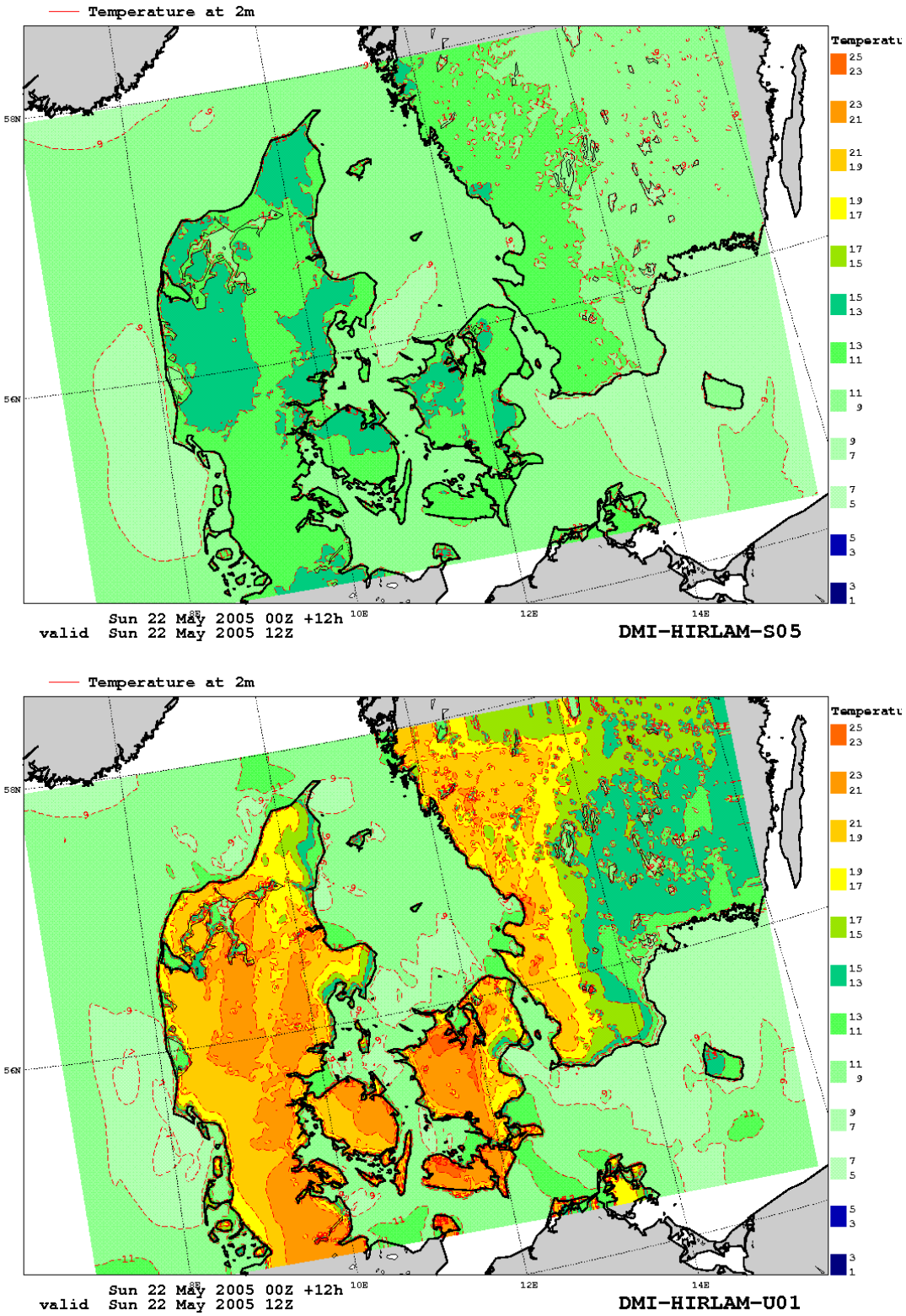

A6.3. Temperature fields at 2 m over the U01 modelling domain simulated by the DMI-HIRLAM-S05 (top) and U01 (bottom) models at term of 12 UTC, 22 May 2005.

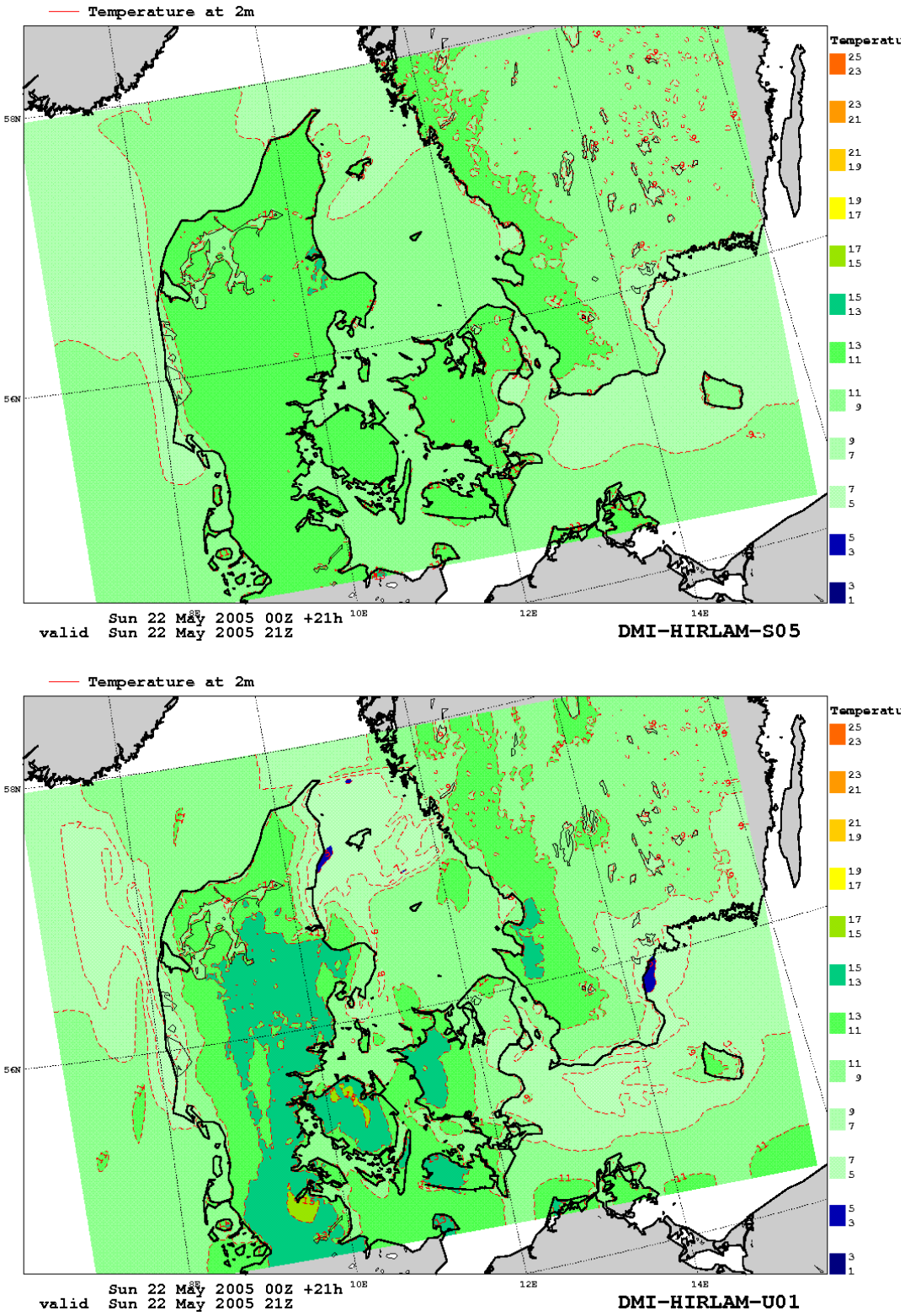

Fig. A6.4. Temperature fields at 2 m over the U01 modelling domain simulated by the DMI-HIRLAM-S05 (top) and U01 (bottom) models at term of 21 UTC, 22 May 2005.

Previous reports

Previous reports from the Danish Meteorological Institute can be found on:
http://www.dmi.dk/dmi/dmi-publikationer.htm